CrossMark

Econometric Theory, **34**, 2018, 447–476.
doi:10.1017/S0266466617000135

SEMI-PARAMETRIC SEASONAL UNIT ROOT TESTS

TOMÁS DEL BARRIO CASTRO
University of the Balearic Islands

PAULO M.M. RODRIGUES
Universidade Nova de Lisboa

A.M. ROBERT TAYLOR
University of Essex

We extend the $\mathcal{M}$ class of unit root tests introduced by Stock (1999, *Cointegration, Causality and Forecasting. A Festschrift in Honour of Clive W.J. Granger*. Oxford University Press), Perron and Ng (1996, *Review of Economic Studies* 63, 435–463) and Ng and Perron (2001, *Econometrica* 69, 1519–1554) to the seasonal case, thereby developing semi-parametric alternatives to the regression-based augmented seasonal unit root tests of Hylleberg, Engle, Granger, and Yoo (1990, *Journal of Econometrics* 44, 215–238). The success of this class of unit root tests to deliver good finite sample size control even in the most problematic (near-cancellation) case where the shocks contain a strong negative moving average component is shown to carry over to the seasonal case as is the superior size/power trade-off offered by these tests relative to other available tests.

1. INTRODUCTION

Augmented Dickey-Fuller [ADF] unit root tests are known to suffer significant size distortions when a near-cancellation region caused by a strong negative moving average behaviour is present in the driving shocks. Although increasing the augmentation lag length can mitigate these distortions, a finite sample trade-off occurs with power under the alternative also decreased the greater the lag length used. In discussing ADF tests, Haldrup and Jansson (2006, p. 267) argue that "… practitioners ought to abandon the use of these tests…" in favour of the $\mathcal{M}$ tests because of "… the excellent size properties and 'nearly' optimal power properties" of the latter. The $\mathcal{M}$ class of tests, proposed in Stock (1999) and further developed by Perron and Ng (1996) and Ng and Perron (2001), account for weak dependence in the shocks via a nonparametric estimate of the long run variance, rather than parametric lag augmentation. Ng and Perron (2001) show that $\mathcal{M}$ tests based on autoregressive spectral density [ASD] estimators implemented

We are grateful to the Editor, Peter Phillips, the Co-Editor, Michael Jansson and two anonymous referees for their helpful and constructive comments. Tomás del Barrio Castro acknowledges financial support from projects ECO2011-23934 and ECO2014-58991-C3-3-R. Address correspondence to Robert Taylor, Essex Business School, University of Essex, Wivenhoe Park, Colchester CO4 3SQ, UK; e-mail: rtaylor@essex.ac.uk.

© Cambridge University Press 2017

https://doi.org/10.1017/S0266466617000135 Published online by Cambridge University Press

with a modified Akaike information criterion [MAIC] to select the lag length perform particularly well even in the presence of strong negative moving average components.

Hylleberg et al. (1990) [HEGY] propose a seasonal generalisation of the ADF unit root test allowing the practitioner to test for unit root behaviour at each of the zero and seasonal frequencies. The HEGY tests, like ADF tests, use parametric lag augmentation, to account for weak dependence in the shocks. However, it has been known since the seminal work of Box and Jenkins (1976) that seasonal time series often display significant negative moving average behaviour at the seasonal lag effecting near cancellation regions at both the zero and seasonal frequencies. ARMA behaviour can also be a manifestation of neglected periodic autoregressive behaviour (see, for example, Ghysels and Osborn, 2001, Chap. 6). The robustness of seasonal unit root tests to moving average behaviour is therefore a matter of significant practical relevance and simulation evidence suggests that, like the ADF tests, the HEGY tests can be badly oversized in the presence of negative moving averages; see, for example, del Barrio Castro, Osborn, and Taylor (2016).

Motivated by these issues and the success of the nonseasonal $\mathcal{M}$ tests, our purpose is to develop a new class of semi-parametric seasonal unit root tests based on the $\mathcal{M}$ testing approach. In the case of tests at the harmonic seasonal frequencies we show that this requires the use of methods based on demodulated processes. The seasonal $\mathcal{M}$-type tests proposed are based on statistics which correct for weak dependence in the shocks using seasonal long run variance estimates, either sum-of-covariances-based or ASD-based, of the spectrum at the zero and seasonal frequencies. Our analysis explicitly allows for the presence of $ARMA$ shocks. We demonstrate that the limiting distributions of our proposed $\mathcal{M}$ statistics are pivotal under both the null hypothesis and under near-integrated alternatives. Where ASD estimators are used, a seasonal analogue of the MAIC criterion of Ng and Perron (2001), developed in del Barrio Castro et al. (2016), can be used to select the lag length, and consistent with the nonseasonal case, we find in a simulation study that the resulting $\mathcal{M}$ tests can deliver significant improvements over augmented HEGY tests.

The remainder of the paper is organised as follows. Section 2 reviews the seasonal model and the seasonal unit root testing framework. Section 3 outlines our proposed class of seasonal $\mathcal{M}$ unit root tests while Section 4 details their large sample properties. Section 5 presents a Monte Carlo comparison of the finite sample properties of the HEGY and seasonal $\mathcal{M}$ tests. Section 6 concludes. Supporting material can be found in a Supplementary Appendix available at Cambridge Journals Online (journals.cambridge.org/ect).

2. THE SEASONAL UNIT ROOT FRAMEWORK

2.1. The Seasonal Model

Consider the univariate seasonal time-series process $\{y_{Sn+s}\}$, observed with constant seasonal periodicity, S, $S \in \{1, 2, \ldots\}$, which satisfies the following data

https://doi.org/10.1017/S0266466617000135 Published online by Cambridge University Press

generating process [DGP]

$$y_{Sn+s} = x_{Sn+s} + \mu_{Sn+s} \tag{2.1a}$$

$$\alpha(L)x_{Sn+s} = u_{Sn+s},\ s = 1-S,\ldots,0,\ \ n = 1,2,\ldots,N, \tag{2.1b}$$

where μ_{Sn+s} is a purely deterministic component, further details on which are given below, and $\alpha(z) := 1 - \sum_{j=1}^{S} \alpha_j^* z^j$, is an $AR(S)$ polynomial in the conventional lag operator, L. In what follows we define the total sample size to be $T := SN$ and the number of harmonic seasonal frequencies to be $S^* := \lfloor (S-1)/2 \rfloor$, where $\lfloor . \rfloor$ denotes the integer part of its argument.

We assume that $\{u_{Sn+s}\}$ in (2.1b) satisfies the following conditions:

Assumption 1. The error term u_{Sn+s} in (2.1b) follows the linear process $u_{Sn+s} = \psi(L)\varepsilon_{Sn+s}$, where ε_{Sn+s} is $IID(0, \sigma_\varepsilon^2)$ with finite fourth order moments and where $\psi(z) := 1 + \sum_{j=1}^{\infty} \psi_j z^j$ satisfies: (i) $\psi(\exp\{\pm \mathrm{i} 2\pi k/S\}) \neq 0$, $k = 0,\ldots,\lfloor S/2 \rfloor$; and (ii) $\sum_{j=1}^{\infty} j|\psi_j| < \infty$.

Assumption 1 ensures that the spectral density function of u_{Sn+s} is bounded, and that it is strictly positive at both the zero and seasonal spectral frequencies, $\omega_k := 2\pi k/S$, $k = 0,\ldots,\lfloor S/2 \rfloor$. Under Assumption 1 the long run variance of u_{Sn+s} may be defined as $\lambda_0^2 := \sigma_\varepsilon^2 \psi(1)^2 = \gamma_0 + 2\sum_{j=1}^{\infty} \gamma_j$, where $\gamma_j := E(u_{Sn+s}u_{Sn+s-j})$, $j = 0,1,\ldots$. Notice that $\lambda_0^2 = 2\pi f_u(0)$, where $f_u(\omega)$ denotes the spectrum of $\{u_{Sn+s}\}$. Analogous quantities can be defined at the Nyquist, $\omega_{S/2} = \pi$, frequency, where S is even, as $\lambda_{S/2}^2 := \sigma_\varepsilon^2 \psi(-1)^2 = \gamma_0 + 2\sum_{j=1}^{\infty} \cos[\pi j]\gamma_j$, and at the seasonal harmonic frequencies, $(\omega_k, 2\pi - \omega_k)$, as $\lambda_k^2 := \sigma_\varepsilon^2(a_k^2 + b_k^2) = \gamma_0 + 2\sum_{j=1}^{\infty} \cos[\omega_k j]\gamma_j$, $k = 1,\ldots,S^*$, where $a_k := \mathcal{I}m(\psi[\exp(\mathrm{i}\omega_k)])$ and $b_k := \mathcal{R}e(\psi[\exp(\mathrm{i}\omega_k)])$, $k = 1,\ldots,S^*$, with $\mathcal{R}e(\cdot)$ and $\mathcal{I}m(\cdot)$ denoting the real and imaginary parts of their arguments, respectively. Notice that $\lambda_{S/2}^2 = 2\pi f_u(\pi)$ and $\lambda_k^2 = 2\pi f_u(2\pi k/S)$, $k = 1,\ldots,S^*$.

For the deterministic component in (2.1a), $\mu_{Sn+s} := \delta' z_{Sn+s,\xi}$, we consider three empirically relevant cases ($\xi = 1,2,3$). Here and in what follows, it is understood that terms relating to frequency π are to be omitted when S is odd and that where reference is made to the Nyquist frequency this is understood only to apply where S is even.

Case 1: Zero and seasonal frequency intercepts: $z_{Sn+s,1} := [1, \cos(2\pi(Sn+s)/S), \sin(2\pi(Sn+s)/S), \ldots, \cos(2\pi S^*(Sn+s)/S), \sin(2\pi S^*(Sn+s)/S), (-1)^{Sn+s}]'$.

Case 2: Zero and seasonal frequency intercepts, zero frequency trend: $z_{Sn+s,2} := [z'_{Sn+s,1}, Sn+s]'$.

Case 3: Zero and seasonal frequency intercepts and trends: $z_{Sn+s,3} := [z'_{Sn+s,1}, (Sn+s)z'_{Sn+s,1}]'$.

Following Elliot, Rothenberg and Stock (1996), Rodrigues and Taylor (2007) and Jansson and Nielsen (2011), the initial conditions, $x_{1-S},\ldots,x_0$, are taken to

https://doi.org/10.1017/S0266466617000135 Published online by Cambridge University Press

be of $o_p(T^{1/2})$. Relaxing this will not alter the limiting null distributions of the test statistics we outline in this paper due to their exact similarity with respect to the initial conditions; see Smith, Taylor, and del Barrio Castro (2009).

2.2. The Seasonal Unit Root Hypotheses

The Sth order polynomial $\alpha(L)$ in (2.1b) can be factorised at the zero and seasonal spectral frequencies, ω_k, $k = 0, \ldots, \lfloor S/2 \rfloor$, so that $\alpha(L) = \prod_{k=0}^{\lfloor S/2 \rfloor} \omega_k(L)$, where $\omega_0(L) := (1 - \alpha_0 L)$ associates the parameter α_0 with the zero frequency ($\omega_0 = 0$), $\omega_k(L) := \{1 - 2[\alpha_k \cos(\omega_k) - \beta_k \sin(\omega_k)]L + (\alpha_k^2 + \beta_k^2)L^2\}$ corresponds to the conjugate (harmonic) seasonal frequencies $(\omega_k, 2\pi - \omega_k)$, with the associated parameters α_k and β_k, $k = 1, \ldots, S^*$, and $\omega_{S/2}(L) := \left(1 + \alpha_{S/2} L\right)$ which associates the $\alpha_{S/2}$ parameter with the Nyquist frequency ($\omega_{S/2} = \pi$).

Our interest centers on testing the $(\lfloor S/2 \rfloor + 1)$ unit root null hypotheses,

$$H_{0,0} : \alpha_0 = 1, \quad H_{0,S/2} : \alpha_{S/2} = 1, \quad H_{0,k} : \alpha_k = 1, \quad \beta_k = 0, \quad k = 1, \ldots, S^* \tag{2.2}$$

such that $H_{0,0}$ corresponds to a unit root at the zero frequency, while $H_{0,S/2}$ yields a unit root at the Nyquist frequency, and finally $H_{0,k}, k = 1, \ldots, S^*$, yields a pair of complex conjugate unit roots at the harmonic seasonal frequencies $(\omega_k, 2\pi - \omega_k)$. Asymptotic power will be considered under the corresponding local hypotheses; i.e.,

$$\begin{aligned} &H_{1,c_j} : \alpha_j = \exp\left(\tfrac{c_j}{T}\right) \cong \left(1 + \tfrac{c_j}{T}\right), \qquad j = 0, S/2, \\ &H_{1,c_k} : \alpha_k = \exp\left(\tfrac{c_k}{T}\right) \cong \left(1 + \tfrac{c_k}{T}\right) \cap \beta_k = 0, \quad k = 1, \ldots, S^*, \end{aligned} \tag{2.3}$$

where c_k, $k = 0, \ldots, \lfloor S/2 \rfloor$ are fixed constants. Under H_{1,c_k} the process $\{y_{Sn+s}\}$ admits either a single root ($k = 0, S/2$) or a pair of complex conjugate roots ($k = 1, \ldots, S^*$) with modulus in the neighbourhood of unity at frequency ω_k. These roots are stable for $c_k < 0$ and explosive for $c_k > 0$. Notice that H_{1,c_k} reduces to $H_{0,k}$ where $c_k = 0$, $k = 0, \ldots, \lfloor S/2 \rfloor$. In what follows, let $\mathbf{c} := (c_0, c_1, \ldots, c_{\lfloor S/2 \rfloor})'$ be the $(\lfloor S/2 \rfloor + 1)$-vector of noncentrality parameters and denote the lag polynomial $\alpha(L)$ under $H_{1,\mathbf{c}} := \cap_{k=0}^{\lfloor S/2 \rfloor} H_{1,c_k}$ as $\Delta_{\mathbf{c}} := 1 - \sum_{j=1}^{S} \alpha_j^{\mathbf{c}} L^j$.

2.3. Seasonal Unit Root Test Regressions

We conclude this section by briefly outlining the regression-based HEGY approach to testing for seasonal unit roots in $\alpha(L)$. A number of objects defined in so doing will also be needed for the subsequent development of our $\mathcal{M}$ seasonal unit root tests in Section 3.

First the data are de-trended to give exact invariance to the parameters characterising μ_{Sn+s} in (2.1a); this step will also be required for the seasonal $\mathcal{M}$ tests. To that end, we define the de-trended data series generically as $y_{Sn+s}^{\xi} := y_{Sn+s} - \hat{\delta}' z_{Sn+s,\xi}$ where $\xi = 1$, 2, and 3 corresponds to the deterministic kernels defined in Cases 1, 2, and 3 above. For OLS de-trending, $\hat{\delta}$ is the OLS estimator

https://doi.org/10.1017/S0266466617000135 Published online by Cambridge University Press

from regressing y_{Sn+s} onto $z_{Sn+s,\xi}$, while, as in Rodrigues and Taylor (2007), for local GLS de-trending $\hat{\delta}$ obtains from the OLS regression of $\mathbf{y_c}$ on $\mathbf{z_{c,\xi}}$, where

$$\begin{aligned}\mathbf{y_c} &:= (y_{1-S}, y_{2-S} - \alpha_1^{\mathbf{c}} y_{1-S}, y_{3-S} - \alpha_1^{\mathbf{c}} y_{2-S} - \alpha_2^{\mathbf{c}} y_{1-S}, \ldots, y_0 - \alpha_1^{\mathbf{c}} y_{-1} \\ &\quad - \cdots - \alpha_S^{\mathbf{c}} y_{1-S}, \Delta_{\mathbf{c}} y_1, \ldots \Delta_{\mathbf{c}} y_T)' \\ \mathbf{z_{c,\xi}} &:= (z_{1-S,\xi}, z_{2-S,\xi} - \alpha_1^{\mathbf{c}} z_{1-S,\xi}, z_{3-S,\xi} - \alpha_1^{\mathbf{c}} z_{2-S,\xi} - \alpha_2^{\mathbf{c}} z_{1-S,\xi}, \ldots, z_{0,\xi} \\ &\quad - \alpha_1^{\mathbf{c}} z_{1,\xi} - \cdots - \alpha_S^{\mathbf{c}} z_{1-S,\xi}, \Delta_{\mathbf{c}} z_{1,\xi}, \ldots, \Delta_{\mathbf{c}} z_{T,\xi})'\end{aligned}$$

for $\mathbf{c} = \bar{\mathbf{c}} := (\bar{c}_0, \bar{c}_1, \ldots, \bar{c}_{\lfloor S/2 \rfloor})'$. The local GLS de-trending parameters, $\bar{c}_k$, $k = 0, \ldots, \lfloor S/2 \rfloor$, are determined by the significance level that the seasonal unit root tests are to be run at and the de-trending scheme employed; see Rodrigues and Taylor (2007, p. 556). For example, under Case 1 for tests run at the 5% level, $\bar{c}_0 = \bar{c}_{S/2} = -7$ and $\bar{c}_k = -3.75$, $k = 1, \ldots, S^*$. The resulting de-trended series satisfies $\alpha(L) y^{\xi}_{Sn+s} = u^{\xi}_{Sn+s}$ with $u^{\xi}_{Sn+s} := \psi(L)\varepsilon^{\xi}_{Sn+s}$, where u^{ξ}_{Sn+s} and ε^{ξ}_{Sn+s} are the correspondingly de-trended versions of u_{Sn+s} and ε_{Sn+s}, respectively.

The HEGY approach then consists of taking an expansion around the zero and seasonal frequency unit roots $\exp(\pm \mathrm{i} 2\pi k/S)$, $k = 0, \ldots, \lfloor S/2 \rfloor$ to obtain the *augmented* HEGY regression:

$$\Delta_S y^{\xi}_{Sn+s} = \sum_{k=0}^{\lfloor S/2 \rfloor} \pi_k y^{\xi}_{k,Sn+s-1} + \sum_{j=1}^{S^*} \pi_j^* y^{*\xi}_{j,Sn+s-1} + \sum_{j=1}^{p^*} \phi_j^* \Delta_S y^{\xi}_{Sn+s-j} + u^{\xi}_{Sn+s,p^*}, \quad \textbf{(2.4)}$$

where $\Delta_S := 1 - L^S$, $y^{\xi}_{k,Sn+s} := \sum_{i=0}^{S-1} \cos[(i+1)\omega_k] y^{\xi}_{Sn+s-i}$, $k = 0, \ldots, \lfloor S/2 \rfloor$, and, $y^{*\xi}_{j,Sn+s-1} := -\sum_{i=0}^{S-1} \sin[(i+1)\omega_j] y^{\xi}_{Sn+s-i}$. An *un-augmented* version of the HEGY regression obtains by setting $p^* = 0$ in (2.4); that is, omitting the lagged dependent variables from the regression.

As outlined in Section S.3 of the accompanying supplement, the so-called HEGY tests for testing $H_{0,0}$, $H_{0,S/2}$ and $H_{0,k}$, $k = 1, \ldots, S^*$, can be formulated as standard t- and F-tests for $\pi_0 = 0$ (denoted t_0), $\pi_{S/2} = 0$ (denoted $t_{S/2}$) and $\pi_k = \pi_k^* = 0$ (denoted F_k), $k = 1, \ldots, S^*$, respectively, in (2.4). Joint tests for $H_0 := \cap_{k=0}^{\lfloor S/2 \rfloor} H_{0,k}$ (denoted $F_{0\ldots\lfloor S/2 \rfloor}$) and $H_{0,\text{seas}} := \cap_{k=1}^{\lfloor S/2 \rfloor} H_{0,k}$ (denoted $F_{1\ldots\lfloor S/2 \rfloor}$) can also be performed. In Section S.5 of the Supplementary Appendix we also detail how the nonseasonal Phillips and Perron (1988) [PP] unit root testing principle can be implemented to test for zero and seasonal frequency unit roots in seasonally observed data based on estimating the un-augmented form of (2.4).

3. $\mathcal{M}$-TYPE SEASONAL UNIT ROOT TESTS

In this section we propose semiparametric seasonal unit root tests based on generalising the nonseasonal $\mathcal{M}$ unit root tests to the seasonal case. In Section 3.1, as background material, we first briefly review the trinity of nonseasonal $\mathcal{M}$ unit root tests.

https://doi.org/10.1017/S0266466617000135 Published online by Cambridge University Press

3.1. Non-Seasonal $\mathcal{M}$ Unit Root Tests

For the nonseasonal ($S = 1$) case, Perron and Ng (1996), Stock (1999) and Ng and Perron (2001) define the trinity of so-called $\mathcal{M}$ unit root test statistics as follows:

$$\mathcal{MZ}_0 := \frac{T^{-1}\left[(y_T^{\xi})^2 - (y_0^{\xi})^2\right] - \hat{\lambda}_0^2}{2T^{-2}\sum_{t=1}^{T}\left(y_{t-1}^{\xi}\right)^2}, \quad \mathcal{MSB}_0 := \left(T^{-2}\sum_{n=1}^{T}\left(y_{t-1}^{\xi}\right)^2/\hat{\lambda}_0^2\right)^{1/2} \tag{3.1}$$

and $\mathcal{MZ}_{t_0} := \mathcal{MZ}_0 \times \mathcal{MSB}_0$, where $\hat{\lambda}_0^2$ is a consistent estimator of the long run variance, λ_0^2. Stock (1999) shows that the first of these statistics, $\mathcal{MZ}_0$, can be re-written[1] as $\mathcal{MZ}_0 = Z_0 + \frac{T}{2}(\hat{\pi}_0)^2$, where $Z_0 := T\hat{\pi}_0 - \frac{(\hat{\lambda}_0^2 - \hat{\gamma}_0)}{2}\left(T^{-2}\sum_{t=1}^{T}\left(y_{t-1}^{\xi}\right)^2\right)^{-1}$ is the nonseasonal coefficient-based PP unit root test, where $\hat{\pi}_0$ and $\hat{\gamma}_0$ are the OLS estimate of π_0 and the OLS residual variance estimate, respectively, from (2.4) with $p^* = 0$ when $S = 1$ (i.e., an un-augmented Dickey-Fuller regression). It can therefore be seen to be a modified version of the PP nonseasonal unit root test statistic, Z_0. These two statistics are asymptotically equivalent under $H_{0,c}$. The second statistic, $\mathcal{MSB}_0$, can be used as a basis for a unit root test by noting that the sums of squares of an $I(1)$ series is of $O_p(T^2)$ while that of an $I(0)$ series is of $O_p(T)$. A test which rejects for small values of the $\mathcal{MSB}_0$ statistic therefore tests the unit root null hypothesis against the stationary alternative. Stock (1999) shows that $\mathcal{MSB}_0$ can be viewed as a modified version of Bhargava's (1986) R_1 statistic. The final test is based on PP's (nonseasonal) t-based unit root statistic $Z_{t_0} := \frac{\hat{\gamma}_0^{1/2}}{\hat{\lambda}_0}t_0 - \frac{(\hat{\lambda}_0^2 - \hat{\gamma}_0)}{2}\left(\hat{\lambda}_0^2 T^{-2}\sum_{t=1}^{T}\left(y_{t-1}^{\xi}\right)^2\right)^{-1/2}$, where t_0 is the t-ratio on π_0 in the un-augmented form of (2.4) when $S = 1$. Noting that $Z_{t_0} = \mathcal{MSB}_0 \times Z_0$, Perron and Ng (1996) propose $\mathcal{MZ}_{t_0}$ as a modified version of the PP Z_{t_0} test. As with the corresponding coefficient-based modified statistics, $\mathcal{MZ}_{t_0}$ and Z_{t_0} are asymptotically equivalent under $H_{0,c}$.

3.2. Zero and Nyquist Frequency $\mathcal{M}$ Unit Root Tests

We now consider how we may generalise the principles underlying the trinity of nonseasonal $\mathcal{M}$ unit root tests outlined above to develop tests for unit roots at the zero and Nyquist frequencies in the seasonal case. Consider first the modified coefficient-type tests. Here, in a similar vein to the relationship that holds between $\mathcal{MZ}_0$ and Z_0 in the nonseasonal case, it is straightforward to show that $\mathcal{MZ}_k = Z_k + \frac{T}{2}(\hat{\pi}_k)^2 + o_p(1)$, $k = 0, S/2$, where for the zero ($k = 0$) and Nyquist ($k = S/2$) frequencies,

$$\mathcal{MZ}_k := \frac{T^{-1}\left[\left(y_{k,T}^{\xi}\right)^2 - \left(y_{k,0}^{\xi}\right)^2\right] - \hat{\lambda}_k^2}{2T^{-2}\sum_{Sn+s=1}^{T}\left(y_{k,Sn+s-1}^{\xi}\right)^2}, \; k = 0, S/2, \tag{3.2}$$

with $\hat{\pi}_k$ the OLS estimates of π_k, $k = 0, S/2$, from estimating (2.4) with $p^* = 0$, Z_0 and $Z_{S/2}$ the zero and Nyquist frequency coefficient-based PP statistics,

https://doi.org/10.1017/S0266466617000135 Published online by Cambridge University Press

respectively, defined in Section S.5 of the Supplementary Appendix. Finally, $\hat{\lambda}^2_0$ and $\hat{\lambda}^2_{S/2}$ are consistent estimators of λ^2_0 and $\lambda^2_{S/2}$, respectively. The unit root null hypothesis at the zero and Nyquist frequencies is rejected for large negative values of the $\mathcal{MZ}_0$ and $\mathcal{MZ}_{S/2}$ statistics, respectively.

To make the $\mathcal{MZ}_k$, $k = 0, S/2$, tests operational we therefore need consistent estimators of the long run variance parameters λ^2_k, $k = 0, S/2$. Following Breitung and Franses (1998) and Gregoir (2006), these can be obtained using sums-of-covariances (or kernel-based) estimators based on the estimated un-augmented form of (2.4), and are defined as follows:

$$\hat{\lambda}^2_{k,WA} := \sum_{j=-T+1}^{T-1} \kappa(j/m)\hat{\gamma}_j \cos(\omega_k j), \qquad k = 0, S/2 \tag{3.3}$$

where $\omega_0 = 0$ and $\omega_{S/2} = \pi$, and $\hat{\gamma}_j$ is the sample autocovariance of order j computed from the OLS residuals from estimating (2.4) setting $p^* = 0$. Analogous quantities at the harmonic seasonal frequencies can be defined as $\hat{\lambda}^2_{k,WA}$, $k = 1, \ldots, S^*$, by setting $\omega_k = 2\pi k/S$ for $k = 1, \ldots, S^*$ in the formula in (3.3). These estimators are consistent under $H_{1,\mathbf{c}}$ provided the kernel function $\kappa(\cdot)$ satisfies e.g., the general conditions reported in Jansson (2002, Assumption A3) and the bandwidth parameter $m \in (0, \infty)$ satisfies the rate condition $1/m + m^2/T \to 0$ as $T \to \infty$ (which corresponds to Assumption A4 of Jansson, 2002).

An alternative approach, which in the nonseasonal case has been shown to deliver unit root tests with considerably better finite sample size properties, is to use the ASD estimators originally proposed in Berk (1974) and extended to the context of the ADF regression by Perron and Ng (1998); see, in particular, Ng and Perron (2001) and Haldrup and Jansson (2006). Following the approach in Berk (1974), the ASD analogues of the sums-of-covariances estimators in (3.3) are given by:

$$\hat{\lambda}^2_{k,AR} := s^2_e \left(1 - \widehat{\phi}(e^{\mathrm{i}\omega_k})\right)^{-2}, \qquad k = 0, S/2. \tag{3.4}$$

Analogous quantities at the harmonic seasonal frequencies can be defined as

$$\hat{\lambda}^2_{k,AR} := \frac{s^2_e}{\left\{1 - \mathcal{R}e\left(\widehat{\phi}\left(e^{(\mathrm{i}\omega_k)}\right)\right)\right\}^2 + \left\{\mathcal{I}m\left(\widehat{\phi}\left(e^{(\mathrm{i}\omega_k)}\right)\right)\right\}^2}, \; k = 1, \ldots, S^*. \tag{3.5}$$

In (3.4) and (3.5), s^2_e and $\widehat{\phi}(L) := \sum_{i=1}^{p^*} \hat{\phi}^*_i L^i$ denote the OLS residual variance estimator and the fitted augmentation polynomial, respectively, from the augmented HEGY regression, (2.4), with $\hat{\phi}^*_j$ denoting the OLS estimator of ϕ^*_j, $j = 1, \ldots, p^*$, from (2.4). Consistency of the ASD estimators under $H_{1,\mathbf{c}}$ requires that: (i) the lag polynomial $\psi(z)$ is invertible, and (ii) that the lag length used in estimating (2.4) satisfies $(1/p^*) + (p^*)^3/T \to 0$ as $T \to \infty$; see Berk (1974).

Noting that the HEGY transformed level variables $y^{\xi}_{0,Sn+s}$ and $y^{\xi}_{S/2,Sn+s}$, defined just below (2.4), filter out unit roots at all but the zero and Nyquist frequency, respectively, the sums of squares of these variables can be used to form

https://doi.org/10.1017/S0266466617000135 Published online by Cambridge University Press

the analogues at the zero and Nyquist frequencies, respectively, of the nonseasonal $\mathcal{MSB}_0$ statistic defined in (3.1); that is,

$$\mathcal{MSB}_k := \left[\frac{1}{T^2 \hat{\lambda}_k^2} \sum_{Sn+s=1}^{T} \left(y_{k,Sn+s-1}^{\xi} \right)^2 \right]^{1/2}, \; k = 0, S/2. \tag{3.6}$$

The unit root null at the zero and Nyquist frequencies is rejected for small values of $\mathcal{MSB}_0$ and $\mathcal{MSB}_{S/2}$, respectively. Combining (3.2) and (3.6), $\mathcal{M}$ versions of the seasonal t-based PP-type Z_{t_k}, $k = 0, S/2$ tests (as defined in Section S.5 of the Supplementary Appendix) can then be straightforwardly defined to reject for small values of the statistics

$$\mathcal{MZ}_{t_k} := \mathcal{MZ}_k \times \mathcal{MSB}_k, \;\; k = 0, S/2. \tag{3.7}$$

3.3. Harmonic and Joint Frequency $\mathcal{M}$ Unit Root Tests

In order to generalise the $\mathcal{M}$ tests to the harmonic seasonal frequencies, we will consider an approach based around the use of the demodulator operator introduced by Granger and Hatanaka (1964) and used in the context of complex unit root analysis by, *inter alia*, Gregoir (1999, 2006).[2]

To illustrate the principle of demodulation, consider the complex-valued process, z_{Sn+s}, near-integrated at frequency ω_k, $(1-(1+\frac{c_k}{T})e^{-\mathrm{i}\omega_k}L)z_{Sn+s} = u_{Sn+s}$, where the innovation u_{Sn+s} satisfies Assumption 1. By recursive substitution it follows that z_{Sn+s} can be written as,

$$z_{Sn+s} = e^{-\mathrm{i}\omega_k(Sn+s)} \left[\left(1+\frac{c_k}{T}\right)^{(Sn+s)} z_0 + \sum_{j=1}^{Sn+s} \left(1+\frac{c_k}{T}\right)^{Sn+s-j} e^{\mathrm{i}\omega_k j} u_j \right]. \tag{3.8}$$

From the representation in (3.8) we observe that z_{Sn+s} is driven by the complex innovation $e^{\mathrm{i}\omega_k j} u_j$ and can be expressed as a complex-valued near-integrated process at the zero frequency multiplied by the demodulator operator $e^{-\mathrm{i}\omega_k(Sn+s)}$. The latter shifts the peak in the spectrum which occurs at the zero frequency with the former to a peak in the spectrum at frequency ω_k.

In order to use the demodulation-based approach to develop harmonic frequency $\mathcal{M}$-type tests we first need to define the demodulated complex conjugate variables,

$$y_{k,Sn+s}^{\xi,\mathrm{D}a} := e^{\mathrm{i}\omega_k(Sn+s)} \left(1 - e^{\mathrm{i}\omega_k} L\right) \Delta_k^0(L)\, y_{Sn+s}^{\xi} \tag{3.9}$$

$$y_{k,Sn+s}^{\xi,\mathrm{D}b} := e^{-\mathrm{i}\omega_k(Sn+s)} \left(1 - e^{-\mathrm{i}\omega_k} L\right) \Delta_k^0(L)\, y_{Sn+s}^{\xi} \tag{3.10}$$

in each case for $k = 1, \ldots, S^*$, where

$$\begin{aligned} \Delta_k^0(L) &:= (1-L)(1+L) \sum_{j \neq k, j=1}^{S^*} (1 - 2\cos[\omega_j] L + L^2) \\ &= \sin[\omega_k]^{-1} \left(\sum_{j=0}^{S-1} \sin[(j+1)\omega_k] L^j \right) \end{aligned} \tag{3.11}$$

https://doi.org/10.1017/S0266466617000135 Published online by Cambridge University Press

omitting the factor $(1+L)$ above when S is odd. As demonstrated in the Supplementary Appendix (see equation (S.17)), applying the filter $\Delta_k^0(L)$ to y_{Sn+s}^{ξ} yields a real-valued near-integrated process at frequency ω_k with associated AR(2) polynomial $(1-2\cos(\omega_k)(1+\frac{c_k}{T})L+(1+\frac{c_k}{T})^2L^2)$. Consequently, the filters $(1-e^{\mathrm{i}\omega_k}L)\Delta_k^0(L)$ and $(1-e^{-\mathrm{i}\omega_k}L)\Delta_k^0(L)$ when applied to y_{Sn+s}^{ξ} deliver the complex-valued near-integrated processes with associated (complex) AR(1) polynomials $(1-(1+\frac{c_k}{T})e^{-\mathrm{i}\omega_k}L)$ and $(1-(1+\frac{c_k}{T})e^{\mathrm{i}\omega_k}L)$, respectively; see (S.18) and (S.19) in the Appendix. Finally, the demodulation by multiplication by $e^{\mathrm{i}\omega_k(Sn+s)}$ and $e^{-\mathrm{i}\omega_k(Sn+s)}$ in (3.9) and (3.10), respectively, yields the complex-valued near-integrated processes at the zero frequency, $y_{k,Sn+s}^{\xi,\mathrm{D}a}$ and $y_{k,Sn+s}^{\xi,\mathrm{D}b}$, associated with the filters $(1-(1+\frac{c_k}{T})e^{-\mathrm{i}\omega_k}L)$ and $(1-(1+\frac{c_k}{T})e^{\mathrm{i}\omega_k}L)$, respectively; see (S.27) and (S.28) in the Supplementary Appendix.

The following weak convergence results for $y_{k,Sn+s}^{\xi,\mathrm{D}a}$ and $y_{k,Sn+s}^{\xi,\mathrm{D}b}$ of (3.9) and (3.10), respectively, follow straightforwardly from (S.27) and (S.28) in the Supplementary Appendix,

$$T^{-1/2}y_{k,S\lfloor rN\rfloor+s}^{\xi,\mathrm{D}a}\Rightarrow\frac{\sigma_\varepsilon\psi\left(e^{\mathrm{i}\omega_k}\right)}{\sqrt{2}}\left[J_{k,c_k}^{\zeta}(r)+\mathrm{i}J_{k,c_k}^{\zeta*}(r)\right]=:\frac{\sigma_\varepsilon\psi\left(e^{\mathrm{i}\omega_k}\right)}{\sqrt{2}}\mathbb{J}_{k,c_k}(r), \tag{3.12}$$

$$T^{-1/2}y_{k,S\lfloor rN\rfloor+s}^{\xi,\mathrm{D}b}\Rightarrow\frac{\sigma_\varepsilon\psi\left(e^{-\mathrm{i}\omega_k}\right)}{\sqrt{2}}\left[J_{k,c_k}^{\zeta}(r)-\mathrm{i}J_{k,c_k}^{\zeta*}(r)\right]=:\frac{\sigma_\varepsilon\psi\left(e^{-\mathrm{i}\omega_k}\right)}{\sqrt{2}}\overline{\mathbb{J}_{k,c_k}(r)}, \tag{3.13}$$

in each case for $k=1,\ldots,S^*$ and where "$\Rightarrow$" denotes weak convergence, as $T\to\infty$, in the Skorohod topology. In (3.12) and (3.13), $\psi(\cdot)$ is as defined in Assumption 1, while $J_{k,c_k}^{\zeta}(r)$ and $J_{k,c_k}^{\zeta*}(r)$, $k=1,\ldots,S^*$, are the independent Ornstein-Uhlenbeck based processes which will subsequently be defined in Theorem 4.1. Notice that $\mathbb{J}_{k,c_k}$ and $\overline{\mathbb{J}_{k,c_k}}$ in (3.12) and (3.13), respectively, form a complex conjugate pair of complex OU processes.

As the limiting representations given for $y_{k,Sn+s}^{\xi,\mathrm{D}a}$ and $y_{k,Sn+s}^{\xi,\mathrm{D}b}$ in (3.12) and (3.13) make clear, developing feasible harmonic frequency $\mathcal{M}$-type test statistics based on these demodulated variables will require taking appropriate real-valued transformations of $y_{k,Sn+s}^{\xi,\mathrm{D}a}$ and $y_{k,Sn+s}^{\xi,\mathrm{D}b}$, together with estimates of the seasonal long run variance nuisance parameters $\sigma_\varepsilon\psi(e^{\mathrm{i}\omega_k})$ and $\sigma_\varepsilon\psi(e^{-\mathrm{i}\omega_k})$ which feature in (3.12) and (3.13), respectively, which are consistent under $H_{1,\mathbf{c}}$. It is straightforward to show that the latter can be obtained, under the conditions stated for consistent estimation in Section 3.2, using the ASD estimators, $\breve{\lambda}_{k,AR}^2:=s_e^2\{1-[\widehat{\phi}(e^{\mathrm{i}\omega_k})]\}^{-2}$ and $\breve{\lambda}_{k,AR}^{*2}:=s_e^2\{1-[\widehat{\phi}(e^{-\mathrm{i}\omega_k})]\}^{-2}$, $k=1,\ldots,S^*$, where s_e^2 and $\widehat{\phi}(\cdot)$ are as defined below (3.5). For the former, we take the following transformations

$$y_{k,Sn+s}^{\mathcal{R}e,\xi}:=\frac{1}{2}\mathcal{R}e\left(\frac{y_{k,Sn+s}^{\xi,\mathrm{D}a}}{\breve{\lambda}_{k,AR}\sqrt{T}}+\frac{y_{k,Sn+s}^{\xi,\mathrm{D}b}}{\breve{\lambda}_{k,AR}^{*}\sqrt{T}}\right), \tag{3.14}$$

$$y_{k,Sn+s}^{\mathcal{I}m,\xi}:=\frac{1}{2}\mathcal{I}m\left(\frac{y_{k,Sn+s}^{\xi,\mathrm{D}a}}{\breve{\lambda}_{k,AR}\sqrt{T}}-\frac{y_{k,Sn+s}^{\xi,\mathrm{D}b}}{\breve{\lambda}_{k,AR}^{*}\sqrt{T}}\right), \tag{3.15}$$

https://doi.org/10.1017/S0266466617000135 Published online by Cambridge University Press

for $k = 1, \ldots, S^*$. Notice that the transformations in (3.14) and (3.15) are designed such that they weakly converge to $J^{\zeta}_{k,c_k}(r)$ and $J^{\zeta *}_{k,c_k}(r)$, respectively. Other transformations with this same asymptotic property could be used instead, but we found little difference even in very small samples compared to using (3.14) and (3.15).

The sequence of transformations in (3.9)–(3.10) and (3.14)–(3.15) map the original (de-trended) series y^{ξ}_{Sn+s} which admits a complex pair of (near-) unit roots at frequency ω_k into two (scaled) series, $y^{\mathcal{R}e,\xi}_{k,Sn+s}$ and $y^{\mathcal{I}m,\xi}_{k,Sn+s}$, each of which has a single (near-) unit root at the zero frequency. Consequently, under $H_{0,k}$ where y^{ξ}_{Sn+s} admits a pair of unit roots at frequency ω_k, then so the two demodulated series $y^{\mathcal{R}e,\xi}_{k,Sn+s}$ and $y^{\mathcal{I}m,\xi}_{k,Sn+s}$ will each contain a zero frequency unit root. Likewise, under H_{1,c_k}, $y^{\mathcal{R}e,\xi}_{k,Sn+s}$ and $y^{\mathcal{I}m,\xi}_{k,Sn+s}$ each admit either a stable ($c_k < 0$) or explosive ($c_k > 0$) root at frequency zero. Consequently, by analogy to the nonseasonal $\mathcal{M}$ tests in Section 3.1, $H_{0,k}$ can therefore be tested against H_{1,c_k} using either $y^{\mathcal{R}e,\xi}_{k,Sn+s}$ or $y^{\mathcal{I}m,\xi}_{k,Sn+s}$ in the following harmonic frequency $\mathcal{M}$-type statistics, in each case for $k = 1, \ldots, S^*$,

$$\mathcal{K}\text{-}\mathcal{MSB}_k := \left[\frac{2}{T} \left(\sum_{Sn+s=1}^{T} y^{\mathcal{K},\xi}_{k,Sn+s-1} \right)^2 \right]^{1/2} \tag{3.16}$$

$$\mathcal{K}\text{-}\mathcal{MZ}_k := \frac{\left(y^{\mathcal{K},\xi}_{k,T}\right)^2 - \left(y^{\mathcal{K},\xi}_{k,0}\right)^2 - 1}{[\mathcal{K}\text{-}\mathcal{MSB}_k]^2} \tag{3.17}$$

$$\mathcal{K}\text{-}\mathcal{MZ}_{t_k} := \mathcal{K}\text{-}\mathcal{MZ}_k \times \mathcal{K}\text{-}\mathcal{MSB}_k \tag{3.18}$$

where setting $\mathcal{K} = \mathcal{R}e$ in (3.16)–(3.18) denotes tests based on $y^{\mathcal{R}e,\xi}_{k,Sn+s}$, while setting $\mathcal{K} = \mathcal{I}m$ denotes the corresponding tests based on $y^{\mathcal{I}m,\xi}_{k,Sn+s}$. In parallel with the $\mathcal{M}$ tests from Section 3.2, $H_{0,k}$ is rejected in favour of H_{1,c_k} for large negative values of $\mathcal{R}e\text{-}\mathcal{MZ}_k$, $\mathcal{I}m\text{-}\mathcal{MZ}_k$, $\mathcal{R}e\text{-}\mathcal{MZ}_{t_k}$, and $\mathcal{I}m\text{-}\mathcal{MZ}_{t_k}$, and for small values of $\mathcal{R}e\text{-}\mathcal{MSB}_k$ and $\mathcal{I}m\text{-}\mathcal{MSB}_k$, $k = 1, \ldots, S^*$.

The harmonic frequency $\mathcal{M}$-type unit root test statistics proposed in (3.16)–(3.18) will be shown in Theorem 4.1 to share the same limiting distributions as the corresponding $\mathcal{M}$-type tests defined for the zero and Nyquist frequencies in Section 3.2. As a result, asymptotic critical values for the tests based on these statistics are as given for the corresponding nonseasonal tests. Moreover, this also implies that their asymptotic local power functions under H_{1,c_k} will be close to the power envelope for testing for a single unit root at either the zero or Nyquist frequency. This is known to lie considerably beneath the power envelope for testing $H_{0,k}$ against H_{1,c_k}; see, for example, Rodrigues and Taylor (2007). Consequently, one could consider joint tests which combine the $\mathcal{M}$-type statistics based on (3.14) and (3.15) in order to increase power. To that end we propose the test which rejects for large values of the following statistic, analogous to the F_k test

https://doi.org/10.1017/S0266466617000135 Published online by Cambridge University Press

statistic of HEGY from Section 2.3:

$$F^{\mathrm{D}}_{\mathcal{M},k} := \frac{1}{2}\left[\left(\mathcal{R}e\text{-}\mathcal{MZ}_{t_{\pi_k}}\right)^2 + \left(\mathcal{I}m\text{-}\mathcal{MZ}_{t_{\pi_k}}\right)^2\right],\ k = 1,\ldots,S^*. \tag{3.19}$$

Similarly, $\mathcal{MZ}$-type analogues of the joint frequency $F_{1,\ldots,\lfloor S/2\rfloor}$ and $F_{0,\ldots,\lfloor S/2\rfloor}$ HEGY tests from Section 2.3 can be formed by rejecting $H_{0,\mathrm{seas}}$ and H_0 for large values of the statistics

$$F^{\mathrm{D}}_{\mathcal{M},1\ldots\lfloor S/2\rfloor} := \frac{1}{S-1}\left[2\sum_{k=1}^{S^*} F^{\mathrm{D}}_{\mathcal{M},k} + \left(\mathcal{MZ}_{t_{\pi_{S/2}}}\right)^2\right] \tag{3.20}$$

and

$$F^{\mathrm{D}}_{\mathcal{M},0\ldots\lfloor S/2\rfloor} := \frac{1}{S}\left[2\sum_{k=1}^{S^*} F^{\mathrm{D}}_{\mathcal{M},k} + \left(\mathcal{MZ}_{t_{\pi_0}}\right)^2 + \left(\mathcal{MZ}_{t_{\pi_{S/2}}}\right)^2\right], \tag{3.21}$$

respectively. Analogous joint tests can also be formed by rejecting $H_{0,k}$, $H_{0,\mathrm{seas}}$ and H_0, respectively, for small values of the $\mathcal{MSB}$-type statistics,

$$\mathcal{MSB}^{\mathrm{D}}_k := \frac{1}{2}\left[(\mathcal{R}e\text{-}\mathcal{MSB}_k)^2 + (\mathcal{I}m\text{-}\mathcal{MSB}_k)^2\right]^{1/2},\ k = 1,\ldots,S^* \tag{3.22}$$

$$\mathcal{MSB}^{\mathrm{D}}_{1\ldots\lfloor S/2\rfloor} := \frac{1}{S-1}\left\{\sum_{k=1}^{S^*}\left[\mathcal{MSB}^{\mathrm{D}}_k\right]^2 + \mathcal{MSB}^2_{S/2}\right\}^{1/2}, \tag{3.23}$$

$$\mathcal{MSB}^{\mathrm{D}}_{0\ldots\lfloor S/2\rfloor} := \frac{1}{S}\left\{\sum_{k=1}^{S^*}\left[\mathcal{MSB}^{\mathrm{D}}_k\right]^2 + \mathcal{MSB}^2_0 + \mathcal{MSB}^2_{S/2}\right\}^{1/2}. \tag{3.24}$$

Remark 3.1. The statistics in (3.19)–(3.24) are based on the approach underlying the corresponding F-type HEGY statistics obtained from (2.4). An alternative is to follow the approach used to develop point optimal seasonal unit root tests in Rodrigues and Taylor (2007), whereby the optimal joint tests are based on the sum of the individual optimal test statistics involved. We define these test statistics as follows, $S^{\mathrm{D}}_{\mathcal{M},k} := \mathcal{R}e\text{-}\mathcal{MZ}_{t_k} + \mathcal{I}m\text{-}\mathcal{MZ}_{t_k}$, $k = 1,\ldots,S^*$, $S^{\mathrm{D}}_{\mathcal{M},1\ldots\lfloor S/2\rfloor} := \sum_{k=1}^{S^*} S^{\mathrm{D}}_{\mathcal{M},k} + \mathcal{MZ}_{t_{S/2}}$ and $S^{\mathrm{D}}_{\mathcal{M},0\ldots\lfloor S/2\rfloor} := \sum_{k=1}^{S^*} S^{\mathrm{D}}_{\mathcal{M},k} + \mathcal{MZ}_{t_0} + \mathcal{MZ}_{t_{S/2}}$, rejecting $H_{0,k}$ for large negative values of $S^{\mathrm{D}}_{\mathcal{M},k}$, $k = 1,\ldots,S^*$, and $H_{0,\mathrm{seas}}$ and H_0 for large negative values of $S^{\mathrm{D}}_{\mathcal{M},1\ldots\lfloor S/2\rfloor}$ and $S^{\mathrm{D}}_{\mathcal{M},0\ldots\lfloor S/2\rfloor}$, respectively.

4. ASYMPTOTIC RESULTS FOR THE $\mathcal{M}$-TYPE SEASONAL UNIT ROOT TESTS

We now provide representations for the limiting distributions of the seasonal $\mathcal{M}$-type unit root statistics from Section 3. Proofs can be found in the

https://doi.org/10.1017/S0266466617000135 Published online by Cambridge University Press

Supplementary Appendix. These are shown to have pivotal limiting distributions whose form coincides with those which obtain for serially uncorrelated shocks. Local asymptotic power functions of these tests, together with the relevant power envelopes, are also reported.

4.1. Limiting Distributions

In Theorem 4.1 we provide limiting representations for the single unit root $\mathcal{M}$-type statistics in (3.2), (3.6) and (3.7) and (3.16)–(3.18). These representations are indexed by the parameter ζ whose value is determined by which of Cases 1–3 of μ_{Sn+s}, as outlined in Section 2.1, holds and the frequency under test. For the zero frequency ω_0 tests: Case 1: $\zeta = 1$; Cases 2 and 3: $\zeta = 2$. For the seasonal frequency ω_k, $k = 1, \ldots, \lfloor S/2 \rfloor$, tests: Cases 1 and 2: $\zeta = 1$; Case 3: $\zeta = 2$.

THEOREM 4.1. *Let y_{Sn+s} be generated by (2.1) under $H_{1,\mathbf{c}}$ and let Assumption 1 hold. Then, as $T \to \infty$:*
(i) for the zero ($k = 0$) and Nyquist ($k = S/2$) frequencies, the single $\mathcal{M}$-type seasonal unit root test statistics in (3.2), (3.6) and (3.7) satisfy,

$$\mathcal{MZ}_k \Rightarrow \left\{ 2 \int_0^1 \left[J^{\zeta}_{k,c_k}(r) \right]^2 dr \right\}^{-1} \left\{ \left[J^{\zeta}_{k,c_k}(1) \right]^2 - 1 \right\}, \quad k = 0, S/2, \tag{4.1}$$

$$\mathcal{MSB}_k \Rightarrow \left\{ \int_0^1 \left[J^{\zeta}_{k,c_k}(r) \right]^2 dr \right\}^{1/2} =: \mathfrak{MSB}^{\zeta}_k, \quad k = 0, S/2, \tag{4.2}$$

$$\mathcal{MZ}_{t_k} \Rightarrow \frac{1}{2} \left\{ \int_0^1 \left[J^{\zeta}_{k,c_k}(r) \right]^2 dr \right\}^{-1/2} \left\{ \left[J^{\zeta}_{k,c_k}(1) \right]^2 - 1 \right\} =: \mathcal{T}^{\zeta}_k, \quad k = 0, S/2; \tag{4.3}$$

(ii) the harmonic frequency single unit root test statistics in (3.16)–(3.18), recalling that $\mathcal{K} = \mathcal{R}e$ relates to statistics based on $y^{\mathcal{R}e,\xi}_{k,Sn+s}$ and $\mathcal{K} = \mathcal{I}m$ relates to the corresponding statistics based on $y^{\mathcal{I}m,\xi}_{k,Sn+s}$, satisfy, in each case for $k = 1, \ldots, S^*$,

$$\mathcal{K}\text{-}\mathcal{MZ}_k \Rightarrow \left\{ 2 \int_0^1 \left[\mathcal{H}^{\zeta}_{k,c_k}(r) \right]^2 dr \right\}^{-1} \left\{ \left[\mathcal{H}^{\zeta}_{k,c_k}(1) \right]^2 - 1 \right\} := \mathcal{K}\text{-}\mathcal{MZ}^{\zeta}_k, \tag{4.4}$$

$$\mathcal{K}\text{-}\mathcal{MSB}_k \Rightarrow \left[\int_0^1 \left[\mathcal{H}^{\zeta}_{k,c_k}(r) \right]^2 dr \right]^{1/2} =: \mathcal{K}\text{-}\mathfrak{MSB}^{\zeta}_k, \tag{4.5}$$

$$\mathcal{K}\text{-}\mathcal{MZ}_{t_k} \Rightarrow \mathcal{K}\text{-}\mathcal{MZ}^{\zeta}_k \times \mathcal{K}\text{-}\mathfrak{MSB}^{\zeta}_k =: \mathcal{K}\text{-}\mathcal{T}^{\zeta}_k, \tag{4.6}$$

where "$\Rightarrow$" denotes weak convergence in the Skorohod topology.

In the above $\mathcal{H}^{\zeta}_{k,c_k}(r) := J^{\zeta}_{k,c_k}(r)$ if $\mathcal{K} = \mathcal{R}e$ and $\mathcal{H}^{\zeta}_{k,c_k}(r) := J^{*\zeta}_{k,c_k}(r)$ if $\mathcal{K} = \mathcal{I}m$, with $J^{\zeta}_{0,c_0}(r)$, $J^{\zeta}_{S/2,c_{S/2}}(r)$, $J^{\zeta}_{k,c_k}(r)$ and $J^{\zeta *}_{k,c_k}(r)$, $k = 1, \ldots, S^*$, $\zeta = 1, 2$, collectively forming a set of S mutually independent scalar Ornstein-Uhlenbeck [OU] processes. These limiting processes are defined as follows.

https://doi.org/10.1017/S0266466617000135 Published online by Cambridge University Press

First let $W_0(r)$, $W_{S/2}(r)$, $W_k(r)$ *and* $W_k^*(r)$, $k = 1, \ldots, S^*$, *be mutually independent standard Brownian motions. Then* $J^{\zeta}_{0,c_0}(r)$, $J^{\zeta}_{S/2,c_{S/2}}(r)$, $J^{\zeta}_{k,c_k}(r)$ *and* $J^{\zeta *}_{k,c_k}(r)$, $k = 1, \ldots, S^*$, *are mutually independent functionals of these Brownian motions whose precise form depends on the de-trending index* ξ *and on whether* y^{ξ}_{Sn+s} *is formed using OLS de-trending or local GLS de-trending. In the case of local GLS de-trending: for* $\zeta = 1$, *these are the standard OU processes* $J^1_{k,c_k}(r) := J_{k,c_k}(r) := \int_0^r \exp(c_k(r-s))dW_k(s)$, $k = 0, \ldots, \lfloor S/2 \rfloor$, *and* $J^{1*}_{k,c_k}(r) := J^*_{k,c_k}(r) := \int_0^r \exp(c_k(r-s))dW^*_k(s)$, $k = 1, \ldots, S^*$; *for* $\zeta = 2$, *they take the form* $J^2_{k,c_k}(r) := J^1_{k,c_k}(r) - r\left\{\frac{(1-\bar{c}_k)J^1_{k,c_k}(1)+\bar{c}_k^2\int_0^1 sJ^1_{k,c_k}(s)ds}{1-\bar{c}_k+\bar{c}_k^2/3}\right\}$, $k = 0, \ldots, \lfloor S/2 \rfloor$, *and* $J^{2*}_{k,c_k}(r) := J^{1*}_{k,c_k}(r) - r\left\{\frac{(1-\bar{c}_k)J^{1*}_{k,c_k}(1)+\bar{c}_k^2\int_0^1 sJ^{1*}_{k,c_k}(s)ds}{1-\bar{c}_k+\bar{c}_k^2/3}\right\}$, $k = 1, \ldots, S^*$. *For OLS de-trending they are de-meaned standard OU processes for* $\zeta = 1$, *so that, for example,* $J^1_{k,c_k}(r) := J_{k,c_k}(r) - \int_0^1 J_{k,c_k}(s)ds$, *while for* $\zeta = 2$ *they are de-trended OU processes, so that, for example,* J^2_{k,c_k} *is the de-meaned and de-trended standard OU process,* $J^2_{k,c_k}(r) := J^1_{k,c_k}(r) - 12\left(r - \frac{1}{2}\right)\int_0^1 \left(s - \frac{1}{2}\right)J^1_{k,c_k}(s)ds$.

Remark 4.1. The limiting distributions given for $\mathcal{MZ}_k$, $k = 0, S/2$, in (4.1), are identical (for a given value of ζ) to and independent of those given for $\mathcal{R}e\text{-}\mathcal{MZ}_k$ and $\mathcal{I}m\text{-}\mathcal{MZ}_k$, $k = 1, \ldots, S^*$, in (4.4). Similarly, the limiting distributions for the $\mathcal{MZ}_{t_k}$, $k = 0, S/2$, statistics of (4.3) are identical (for a given value of ζ) to and independent of those for $\mathcal{R}e\text{-}\mathcal{MZ}_{t_k}$ and $\mathcal{I}m\text{-}\mathcal{MZ}_{t_k}$ in (4.6). Moreover, it is also seen from (4.2) and (4.5) that the limiting distributions of the $\mathcal{MSB}_k$, $k = 0, S/2$, $\mathcal{R}e\text{-}\mathcal{MSB}_k$ and $\mathcal{I}m\text{-}\mathcal{MSB}_k$, $k = 1, \ldots, S^*$, statistics are identical (again for a given value of ζ) and are mutually independent.

Remark 4.2. The limiting distributions of the seasonal $\mathcal{M}$-type statistics given in Theorem 4.1 coincide with those of the corresponding nonseasonal $\mathcal{M}$ statistics discussed in Section 3.1, and, hence, are free of any nuisance parameters arising from weak dependence in u_{Sn+s}. Selected critical values for the tests based on these statistics can therefore be obtained from Table I of Elliott, Rothenberg, and Stock (1996, p. 825) and from Table 1 of Ng and Perron (2001, p. 1524). Moreover, the asymptotic local power functions of these statistics also coincide with those given for the corresponding statistics in the nonseasonal case and graphed in Figures 1–3 of Elliott et al. (1996, pp. 822–824). Finally, the representations for $\mathcal{MZ}_{t_0}$ and $\mathcal{MZ}_{t_{S/2}}$ coincide with those given in Rodrigues and Taylor (2007) for the corresponding HEGY statistics t_0 and $t_{S/2}$, respectively.

We now detail the limiting distributions of the joint $\mathcal{M}$ tests from Section 3.

COROLLARY 4.1. *Let the conditions of Theorem 4.1 hold. Then, as* $T \to \infty$:
(*i*) $F^{\mathrm{D}}_{\mathcal{M},k} \Rightarrow \frac{1}{2}\left[\left(\mathcal{R}e\text{-}\mathcal{T}^{\zeta}_k\right)^2 + \left(\mathcal{I}m\text{-}\mathcal{T}^{\zeta}_k\right)^2\right] =: \mathcal{F}^{\mathrm{D},\zeta}_{\mathcal{M},k}$, $k = 1, \ldots, S^*$, $F^{\mathrm{D}}_{\mathcal{M},1\ldots\lfloor S/2 \rfloor} \Rightarrow \frac{1}{S-1}\left[2\sum_{k=1}^{S^*}\mathcal{F}^{\mathrm{D},\zeta}_{\mathcal{M},k} + \left(\mathcal{T}^{\zeta}_{S/2}\right)^2\right]$; $F^{\mathrm{D}}_{\mathcal{M},0\ldots\lfloor S/2 \rfloor} \Rightarrow \frac{1}{S}\left[2\sum_{k=1}^{S^*}\mathcal{F}^{\mathrm{D},\zeta}_{\mathcal{M},k} + \left(\mathcal{T}^{\zeta}_0\right)^2 + \left(\mathcal{T}^{\zeta}_{S/2}\right)^2\right]$;
(*ii*) $\mathcal{MSB}^{\mathrm{D}}_k \Rightarrow \frac{1}{2}\left[\left(\mathcal{R}e\text{-}\mathfrak{MSB}^{\zeta}_k\right)^2 + \left(\mathcal{I}m\text{-}\mathfrak{MSB}^{\zeta}_k\right)^2\right]^{1/2} =: \mathfrak{MSB}^{\mathrm{D},\zeta}_k$,

https://doi.org/10.1017/S0266466617000135 Published online by Cambridge University Press

$k = 1, \ldots, S^*$; $\mathcal{MSB}^{\mathrm{D}}_{j\ldots\lfloor S/2\rfloor} \Rightarrow \left[\sum_{k=j}^{S^*}\left(\mathfrak{MSB}^{\mathrm{D},\zeta}_k\right)^2 + \left(\mathfrak{MSB}^{\zeta}_0\right)^2 + \left(\mathfrak{MSB}^{\zeta}_{S/2}\right)^2\right]^{1/2}$, $j = 0, 1$; *and* (*iii*) $S^{\mathrm{D}}_{\mathcal{M},k} \Rightarrow \mathcal{R}e\text{-}\mathcal{T}^{\zeta}_k + \mathcal{I}m\text{-}\mathcal{T}^{\zeta}_k$, $k = 1, \ldots, S^*$, $S^{\mathrm{D}}_{\mathcal{M},1\ldots\lfloor S/2\rfloor} \Rightarrow \sum_{k=1}^{S^*}\left(\mathcal{R}e\text{-}\mathcal{T}^{\zeta}_k + \mathcal{I}m\text{-}\mathcal{T}^{\zeta}_k\right) + \mathcal{T}^{\zeta}_{S/2}$, *and* $S^{\mathrm{D}}_{\mathcal{M},0\ldots\lfloor S/2\rfloor} \Rightarrow \sum_{k=1}^{S^*}\left(\mathcal{R}e\text{-}\mathcal{T}^{\zeta}_k + \mathcal{I}m\text{-}\mathcal{T}^{\zeta}_k\right) + \mathcal{T}^{\zeta}_0 + \mathcal{T}^{\zeta}_{S/2}$.

Remark 4.3. The limiting distributions which appear in Corollary 4.1 have not appeared in the literature before. Consequently, in Table 1 for the $\mathcal{S}^{\mathrm{D}}_{\mathcal{M}}$ and $\mathcal{MSB}^{\mathrm{D}}$ tests, and in Table 2 for the $F^{\mathrm{D}}_{\mathcal{M}}$ tests, we provide selected asymptotic null critical values, for each of Cases 1–3 for the deterministic component, computed by direct simulation of the relevant limiting null distributions in Corollary 4.1, using 100,000 Monte Carlo replications and a discretisation of $N = 1,000$ steps, for versions of the statistics based on either OLS de-trended data or local GLS de-trended data, the latter using the relevant values of $\bar{c}$ detailed in Section 2.3.

4.2. Asymptotic Local Power Functions

Figures 1 and 2 graph the asymptotic local power functions of the seasonal $\mathcal{M}$-type unit root tests proposed in Section 3, together with the seasonal point optimal-based tests of Rodrigues and Taylor (2007) and, where relevant, the HEGY tests of Section 2.3.[3] All of the tests considered are based on a nominal 5% level. Results for the zero, Nyquist and harmonic frequency unit root tests (which are independent of the seasonal aspect, S) are given in Figure 1, while results for joint frequency tests for the quarterly case, $S = 4$, are given in Figure 2. All results relate to tests based on local GLS de-trended data,

TABLE 1. Asymptotic critical values for the $\mathcal{MSB}^{\mathrm{D}}$-type and $S^{\mathrm{D}}_{\mathcal{M}}$-type tests

	Case 1				Case 2				Case 3			
	0.010	0.025	0.050	0.100	0.010	0.025	0.050	0.100	0.010	0.025	0.050	0.100
OLS de-trended												
$\mathcal{MSB}^{\mathrm{D}}_1$	0.140	0.153	0.166	0.182	0.140	0.153	0.166	0.182	0.111	0.118	0.125	0.134
$\mathcal{MSB}^{\mathrm{D}}_{12}$	0.259	0.280	0.301	0.327	0.259	0.280	0.301	0.327	0.200	0.212	0.223	0.237
$\mathcal{MSB}^{\mathrm{D}}_{012}$	0.363	0.390	0.416	0.449	0.333	0.355	0.376	0.402	0.274	0.289	0.302	0.319
$\mathcal{S}^{\mathrm{D}}_{\mathcal{M}.1}$	−5.733	−5.312	−4.953	−4.541	−5.733	−5.312	−4.953	−4.541	−6.825	−6.419	−6.079	−5.691
$\mathcal{S}^{\mathrm{D}}_{\mathcal{M}.12}$	−7.904	−7.377	−6.939	−6.426	−7.904	−7.377	−6.939	−6.426	−9.576	−9.073	−8.653	−8.175
$\mathcal{S}^{\mathrm{D}}_{\mathcal{M}.012}$	−9.944	−9.347	−8.833	−8.250	−10.504	−9.920	−9.436	−8.847	−12.23	−11.636	−11.164	−10.615
Local GLS de-trended												
$\mathcal{MSB}^{\mathrm{D}}_1$	0.176	0.197	0.219	0.250	0.176	0.197	0.219	0.250	0.125	0.135	0.144	0.156
$\mathcal{MSB}^{\mathrm{D}}_{12}$	0.330	0.368	0.402	0.451	0.333	0.369	0.405	0.453	0.224	0.239	0.253	0.271
$\mathcal{MSB}^{\mathrm{D}}_{012}$	0.474	0.519	0.565	0.624	0.415	0.453	0.488	0.533	0.308	0.327	0.344	0.366
$\mathcal{S}^{\mathrm{D}}_{\mathcal{M}.1}$	−3.951	−3.506	−3.115	−2.648	−3.951	−3.506	−3.115	−2.648	−5.758	−5.350	−5.025	−4.642
$\mathcal{S}^{\mathrm{D}}_{\mathcal{M}.12}$	−5.197	−4.624	−4.168	−3.596	−5.197	−4.623	−4.167	−3.596	−8.012	−7.512	−7.106	−6.647
$\mathcal{S}^{\mathrm{D}}_{\mathcal{M}.012}$	−6.307	−5.679	−5.137	−4.496	−7.245	−6.648	−6.121	−5.519	−10.136	−9.603	−9.134	−8.614

Notes: Case 1 indicates that the deterministic component used consists of a zero and seasonal frequency intercepts; Case 2 indicates that zero and seasonal frequency intercepts and a zero frequency trend were used; and Case 3 indicates that zero and seasonal frequency intercepts and trends were used.

https://doi.org/10.1017/S0266466617000135 Published online by Cambridge University Press

TABLE 2. Asymptotic critical values for the $F^{\mathrm{D}}_{\mathcal{M}}$-type tests

	Case 1				Case 2				Case 3			
	0.900	0.950	0.975	0.990	0.900	0.950	0.975	0.990	0.900	0.950	0.975	0.990
OLS de-trended												
$F^{\mathrm{D}}_{\mathcal{M}.1}$	5.540	6.555	7.496	8.648	5.540	6.555	7.496	8.648	8.420	9.615	10.667	12.028
$F^{\mathrm{D}}_{\mathcal{M}.12}$	5.087	5.867	6.592	7.498	2.333	2.869	3.384	4.064	7.847	8.778	9.607	10.682
$F^{\mathrm{D}}_{\mathcal{M}.012}$	6.403	7.278	8.083	9.063	7.338	8.261	9.081	10.069	10.010	11.039	11.967	13.182
Local GLS de-trended												
$F^{\mathrm{D}}_{\mathcal{M}.1}$	2.555	3.259	3.961	4.880	2.555	3.259	3.961	4.880	5.731	6.695	7.565	8.765
$F^{\mathrm{D}}_{\mathcal{M}.12}$	2.352	2.880	3.414	4.052	2.333	2.869	3.384	4.064	5.343	6.089	6.782	7.648
$F^{\mathrm{D}}_{\mathcal{M}.012}$	2.208	2.647	3.073	3.616	3.956	4.620	5.249	6.035	5.099	5.723	6.318	7.016

Note: See notes to Table 1.

with results given for $\zeta = 1$ and $\zeta = 2$, where the index ζ is as defined immediately prior to Theorem 4.1. The local GLS de-trending parameters $\bar{c}_k$ detailed in Section 2.3 were used for all tests. Each graph also reports the relevant Gaussian asymptotic local power envelope, taken from either Elliott et al. (1996) or Rodrigues and Taylor (2007), as a benchmark. The local power functions were calculated using direct simulation methods with 80,000 Monte Carlo replications, discretising over $N = 1,000$ steps. The horizontal axes of the graphs are indexed by c which is used generically to denote either the relevant frequency-specific noncentrality parameter, c_k, $k = 0, \ldots, \lfloor S/2 \rfloor$ (so that for tests at the zero frequency, for example, $c = c_0$) or, in the case of joint frequency tests, a common noncentrality parameter (for example, $c = c_1 = c_2$ in the case of the tests of the null hypothesis of unit roots at all of the seasonal frequencies).

Consider first Figures 1(a) and 1(b) which pertain to the zero and Nyquist frequency tests. Results are reported for the $\mathcal{M}Z_k$, $\mathcal{M}Z_{t_k}$, and $\mathcal{MSB}_k$, $k = 0, S/2$, tests from Section 3.2 together with the feasible point optimal-type tests from Section 4 of Rodrigues and Taylor (2007, pp. 556–558), denoted $P_{k,T}$, $k = 0, S/2$, in what follows.[4] As discussed in Section 4, for a given value of ζ the large sample behaviour of a given zero frequency statistic and its Nyquist frequency analogue coincide, and coincide with the behaviour of that statistic in the nonseasonal ($S = 1$) case. This is also true of the $P_{k,T}$, $k = 0, S/2$, statistics, as demonstrated in Rodrigues and Taylor (2007). For the local GLS de-meaning ($\zeta = 1$) case in Figure 1(a) it is seen that the asymptotic local power functions of the $\mathcal{M}Z_k$, $\mathcal{M}Z_{t_k}$, $\mathcal{MSB}_k$ and $P_{k,T}$, $k = 0, S/2$ tests all lie very close to the Gaussian power envelope and are almost indistinguishable from each other, echoing results in Figures 1–3 of Elliott et al. (1996). For the local GLS de-trended ($\zeta = 2$) case in Figure 1(b), we see a decline in the power curves and the power envelope relative to the corresponding quantities in Figure 1(a), again consonant with Figures 1–3 of Elliott et al. (1996). In the local GLS de-trended case the tests again all lie very close to one another and again are effectively indistinguishable from the Gaussian power envelope.

https://doi.org/10.1017/S0266466617000135 Published online by Cambridge University Press

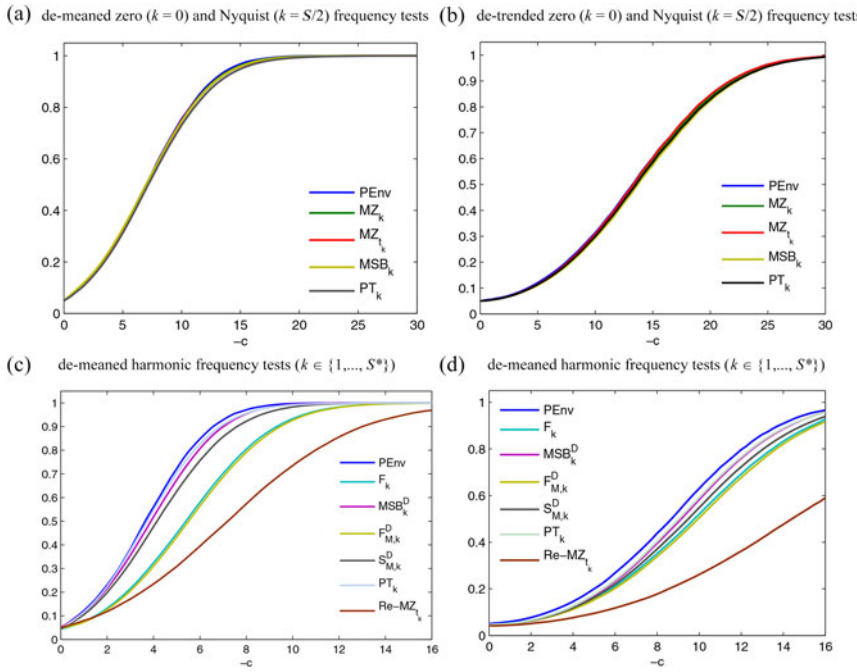


FIGURE 1. Gaussian asymptotic local power envelopes and asymptotic local power functions of zero, Nyquist and harmonic frequency local GLS de-trended unit root tests.

Figures 1(c) and 1(d) present the corresponding results for the harmonic frequency $\mathcal{M}$-type tests of Section 3.3, the feasible point optimal $P_{k,T}$ test of Rodrigues and Taylor (2007) and the HEGY F_k test. Gaussian local power envelopes are from Gregior (2006) and Rodrigues and Taylor (2007). For a given value of ζ, the demodulated single unit root $\mathcal{M}$-type tests in (3.2)–(3.7) and (3.16)–(3.18) were virtually indistinguishable and so we only plot $\mathcal{R}e\text{-}\mathcal{M}\mathcal{Z}_{t_k}$. The results for $\zeta = 1$ in Figure 1(c) show that the local power function of the demodulated $\mathcal{R}e\text{-}\mathcal{M}\mathcal{Z}_{t_k}$ test lies well below both the Gaussian local power envelope and the power functions of the other harmonic frequency unit root tests, as would be expected given that each of the latter jointly test on both complex conjugate harmonic frequency unit roots. Of the other tests, the $P_{k,T}$ test displays the best power. The $\mathcal{M}\mathcal{S}\mathcal{B}^{\mathrm{D}}_k$ and the $S^{\mathrm{D}}_{\mathcal{M},k}$ test of Remark 3.1 are both slightly less powerful than the aforementioned test, followed by the standard HEGY F_k test and the demodulated $F^{\mathrm{D}}_{\mathcal{M},1}$ test whose power functions lie close to one another. The results for $\zeta = 2$ in Figure 1(d) show the same power ordering among the tests as was seen in Figure 1(c) but the differences between these power functions are far less pronounced, with the exception of the demodulated $\mathcal{R}e\text{-}\mathcal{M}\mathcal{Z}_{t_k}$ test whose power function still lies well below those of the other tests. As with the corresponding results in Figures 1(a) and 1(b),

https://doi.org/10.1017/S0266466617000135 Published online by Cambridge University Press

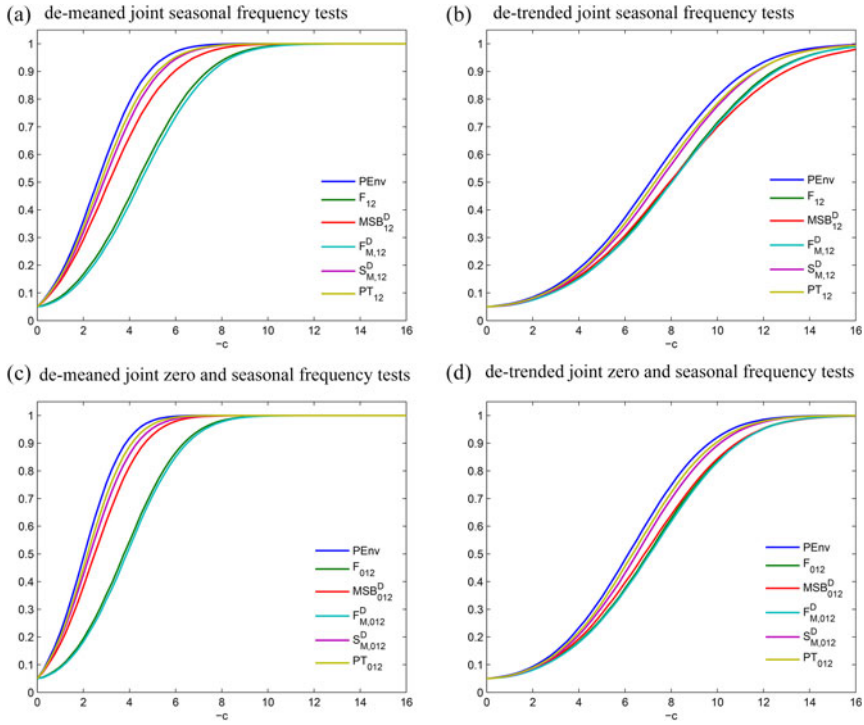


FIGURE 2. Gaussian asymptotic local power envelopes and asymptotic local power functions of joint frequency local GLS de-trended unit root tests for the quarterly case ($S = 4$).

the power functions and the power envelope again decline relative to those in Figure 1(c).

Finally in Figure 2 we graph the Gaussian power envelopes and asymptotic local power functions of the joint frequency tests discussed in this paper which obtain in the quarterly case, $S = 4$. Specifically, Figures 2(a) and 2(b) report results, for the local GLS de-meaned and de-trended cases respectively, for the F_{12}, $F^{\mathrm{D}}_{\mathcal{M},12}$, $\mathcal{MSB}^{\mathrm{D}}_{12}$ and $S^{\mathrm{D}}_{\mathcal{M},12}$ tests and the corresponding feasible point optimal test of Rodrigues and Taylor (2007), denoted $PT_{12,T}$, while Figures 2(c) and 2(d) report results, again for the local GLS de-meaned and de-trended cases respectively, for the F_{012}, $F^{\mathrm{D}}_{\mathcal{M},012}$, $\mathcal{MSB}^{\mathrm{D}}_{012}$, $S^{\mathrm{D}}_{\mathcal{M},012}$ and $PT_{012,T}$ tests, the latter again denoting the relevant feasible point optimal test from Rodrigues and Taylor (2007). Consider first Figures 2(a) and 2(b) which pertain to tests of the null hypothesis of unit roots at all of the seasonal frequencies, $H_{0,\mathrm{seas}} = \cap_{k=1}^{2} H_{0,k}$. The $S^{\mathrm{D}}_{\mathcal{M},12}$ test and the feasible point optimal $P_{12,T}$ test outperform the other tests regardless of whether de-meaning or de-trending is considered. For the de-meaned case, the $\mathcal{MSB}^{\mathrm{D}}_{12}$ test outperforms both the F_{12} and $F^{\mathrm{D}}_{\mathcal{M},12}$ tests, but for the de-trended case these three tests all perform quite similarly. Qualitatively

https://doi.org/10.1017/S0266466617000135 Published online by Cambridge University Press

similar patterns are observed in Figures 2(c) and 2(d) for the corresponding tests of the overall null hypothesis, $H_0 = \cap_{k=0}^{2} H_{0,k}$.

5. FINITE SAMPLE RESULTS

We next investigate the finite sample size and (local) power properties of the new seasonal $\mathcal{M}$-type unit root tests of Section 3, comparing them with the augmented HEGY tests of Section 2.3 and the feasible point optimal tests of Rodrigues and Taylor (2007). Our simulations are based on the following quarterly ($S = 4$) DGP:

$$\left(1 - \left[1 + \frac{c_0}{4N}\right]L\right)\left(1 + \left[1 + \frac{c_2}{4N}\right]L\right)\left(1 + \left[1 + \frac{c_1}{4N}\right]^2 L^2\right) x_{4n+s} = u_{4n+s} \quad \textbf{(5.1)}$$

for $s = -3, \ldots, 0$, $n = 1, \ldots, N$ initialised at $x_{-3} = \cdots = x_0 = 0$, and where u_{4n+s} a stationary error whose properties will be detailed below. Results relating to finite sample size, where $c_0 = c_1 = c_2 = 0$, are reported in Section 5.1, while finite sample power results, where $c_i < 0$, for some $i \in \{0, 1, 2\}$, are reported in Section 5.2. Results are reported for $N = 50$ and $N = 100$.

For the long run variance estimates needed to implement both the new semi-parametric tests proposed in this paper and the corresponding feasible point optimal tests of Rodrigues and Taylor (2007), we explored both sums-of-covariances estimators based on Bartlett and Quadratic Spectral kernels and ASD estimators. Tests based on the latter displayed considerably better finite sample behaviour throughout and so we only report these results. The AR lag order used in constructing the ASD estimates was determined using the seasonal MAIC criterion of del Barrio Castro et al. (2016) using Schwert's rule, $k_{\max K} := \lfloor K[\frac{4N}{100}]^{1/4} \rfloor$, with K a constant discussed below, to determine the maximum lag length allowed. As in Perron and Qu (2007) the MAIC criterion is computed based on OLS de-trended data. Results are reported for both Case 1 (zero and seasonal frequency intercepts) and Case 3 (zero and seasonal frequency intercepts and trends). All reported results are based on local GLS de-trending.

5.1. Empirical Size

In order to explore the impact of near cancellation regions on the finite sample size, Tables 3–5 report results for the case where u_{4n+s} in (5.1) follows the MA(q) process $u_{4n+s} = \varepsilon_{4n+s} - \theta_q \varepsilon_{4n+s-q}$, with $\varepsilon_{4n+s} \sim NIID(0, 1)$, for $s = -3, \ldots, 0$, $n = 1, \ldots, N$, initialised at $\varepsilon_j = 0$, $j \leq 0$. The MA order and range of values of the MA parameter which generate a near cancellation region vary according to the frequency of interest. For the zero frequency we consider $q = 1$ and $\theta_1 \in \{0, 0.2, 0.4, 0.6, 0.8, 0.9\}$. For the Nyquist frequency we consider $q = 1$ and $\theta_1 \in \{0, -0.2, -0.4, -0.6, -0.8, -0.9\}$. For the harmonic frequency, we consider $q = 2$ and $\theta_2 \in \{0, -0.04, -0.16, -0.36, -0.64, -0.81\}$. Notice that the moduli of the resulting MA roots is the same in each design. Given the values of θ_q considered, we set $K = 12$ in the formula for $k_{\max K}$ to allow for a reasonably long lag length in the AR approximation. All tests are run at the nominal asymptotic 5% level.

https://doi.org/10.1017/S0266466617000135 Published online by Cambridge University Press

TABLE 3. Empirical size of zero frequency unit root tests. MAIC lag selection

DGP (5.1) with $c = 0$ and $u_{4n+s} = \varepsilon_{4n+s} - \theta_1 \varepsilon_{4n+s-1}$

Case 1: Local GLS de-trended data

N	θ_1	t_0	$\mathcal{MZ}_0$	$\mathcal{MZ}_{t_0}$	$\mathcal{MSB}_0$	$P_{0.T}$	F_{012}	$F^{\mathrm{D}}_{\mathcal{M}.012}$	$\mathcal{MSB}^{\mathrm{D}}_{012}$	$P_{012.T}$	$S^{\mathrm{D}}_{\mathcal{M}.012}$
50	0.0	0.068	0.079	0.083	0.077	0.067	0.065	0.064	0.117	0.042	0.115
	0.2	0.073	0.094	0.098	0.087	0.079	0.068	0.064	0.119	0.046	0.111
	0.4	0.086	0.105	0.111	0.100	0.091	0.075	0.069	0.123	0.046	0.108
	0.6	0.102	0.108	0.115	0.100	0.096	0.076	0.073	0.131	0.051	0.116
	0.8	0.133	0.062	0.069	0.053	0.064	0.086	0.068	0.099	0.043	0.105
	0.9	0.227	0.081	0.086	0.074	0.082	0.151	0.102	0.061	0.027	0.110
100	0.0	0.063	0.066	0.069	0.064	0.061	0.060	0.052	0.073	0.034	0.072
	0.2	0.064	0.073	0.073	0.073	0.065	0.056	0.054	0.079	0.032	0.069
	0.4	0.070	0.079	0.079	0.077	0.074	0.057	0.057	0.077	0.036	0.072
	0.6	0.079	0.078	0.080	0.077	0.072	0.060	0.060	0.076	0.033	0.075
	0.8	0.103	0.046	0.050	0.040	0.050	0.070	0.050	0.071	0.032	0.069
	0.9	0.182	0.028	0.031	0.025	0.032	0.109	0.056	0.048	0.024	0.066

Case 3: Local GLS de-trended data

N	θ_1	t_0	$\mathcal{MZ}_0$	$\mathcal{MZ}_{t_0}$	$\mathcal{MSB}_0$	$P_{0.T}$	F_{012}	$F^{\mathrm{D}}_{\mathcal{M}.012}$	$\mathcal{MSB}^{\mathrm{D}}_{012}$	$P_{012.T}$	$S^{\mathrm{D}}_{\mathcal{M}.012}$
50	0.0	0.045	0.042	0.045	0.049	0.040	0.067	0.026	0.039	0.019	0.033
	0.2	0.053	0.059	0.065	0.067	0.057	0.069	0.028	0.038	0.019	0.033
	0.4	0.063	0.079	0.084	0.088	0.076	0.069	0.025	0.033	0.015	0.027
	0.6	0.079	0.080	0.084	0.089	0.074	0.092	0.034	0.031	0.017	0.037
	0.8	0.117	0.063	0.067	0.071	0.059	0.121	0.042	0.015	0.010	0.035
	0.9	0.232	0.137	0.140	0.145	0.133	0.205	0.101	0.006	0.003	0.062
100	0.0	0.042	0.040	0.041	0.041	0.046	0.057	0.032	0.042	0.021	0.036
	0.2	0.045	0.051	0.052	0.051	0.056	0.056	0.031	0.043	0.021	0.036
	0.4	0.060	0.065	0.067	0.063	0.072	0.061	0.034	0.043	0.020	0.038
	0.6	0.065	0.056	0.059	0.057	0.065	0.067	0.042	0.051	0.026	0.048
	0.8	0.082	0.020	0.022	0.019	0.027	0.077	0.034	0.023	0.013	0.033
	0.9	0.165	0.023	0.025	0.022	0.029	0.127	0.041	0.007	0.005	0.033

Notes: Case 1 indicates that the deterministic component used consists of zero and seasonal frequency intercepts; Case 3 indicates that zero and seasonal frequency intercepts and trends were used.

Consider first the results in Table 3 for zero frequency tests. Although the standard HEGY t_0 test displays reasonably good size control both when $\theta_1 = 0$ and when θ_1 is small, its empirical size rises significantly above the nominal level as θ_1 increases. This occurs in both Cases 1 and 3, with the distortions slightly lower in general under Case 3. Although ameliorated as N increases, the empirical size of t_0 remains uncomfortably large, even for $N = 100$, for large values of θ_1. To illustrate, under Case 1 and $\theta_1 = 0.9$ the empirical size of t_0 is almost 23% for $N = 50$ reducing only to 18% for $N = 100$. Consistent with findings for the nonseasonal case in Ng and Perron (2001), the trinity of zero frequency $\mathcal{M}$-type tests all display

https://doi.org/10.1017/S0266466617000135 Published online by Cambridge University Press

https://doi.org/10.1017/S0266466617000135 Published online by Cambridge University Press

TABLE 4. Empirical size of Nyquist frequency unit root tests. MAIC lag selection

DGP (5.1) with $c = 0$ and $u_{4n+s} = \varepsilon_{4n+s} + \theta_1 \varepsilon_{4n+s-1}$

Local GLS de-trended data; Case 1 (zero and seasonal frequency intercepts)

N	θ_1	t_2	$\mathcal{MZ}_2$	$\mathcal{MZ}_{t_2}$	$\mathcal{MSB}_2$	$P_{2.T}$	$P_{12.T}$	$P_{012.T}$	F_{12}	F_{012}	$F^{D}_{\mathcal{M}.12}$	$F^{D}_{\mathcal{M}.012}$	$\mathcal{MSB}^{D}_{12}$	$\mathcal{MSB}^{D}_{012}$	$S^{D}_{\mathcal{M}.12}$	$S^{D}_{\mathcal{M}.012}$
50	0.0	0.067	0.081	0.085	0.075	0.067	0.041	0.051	0.068	0.073	0.063	0.070	0.092	0.121	0.060	0.118
	0.2	0.075	0.097	0.103	0.092	0.080	0.043	0.047	0.065	0.070	0.057	0.065	0.093	0.116	0.056	0.106
	0.4	0.082	0.105	0.108	0.101	0.089	0.042	0.048	0.063	0.072	0.060	0.070	0.096	0.123	0.058	0.110
	0.6	0.100	0.103	0.111	0.097	0.092	0.050	0.051	0.070	0.077	0.067	0.076	0.108	0.129	0.067	0.117
	0.8	0.131	0.063	0.068	0.055	0.062	0.044	0.046	0.092	0.094	0.066	0.076	0.079	0.096	0.067	0.115
	0.9	0.216	0.078	0.080	0.072	0.079	0.036	0.028	0.153	0.151	0.086	0.097	0.060	0.055	0.071	0.108
100	0.0	0.062	0.070	0.069	0.068	0.063	0.030	0.032	0.056	0.056	0.056	0.054	0.063	0.073	0.040	0.068
	0.2	0.065	0.074	0.076	0.073	0.068	0.035	0.030	0.055	0.055	0.050	0.055	0.069	0.077	0.043	0.072
	0.4	0.072	0.081	0.082	0.079	0.073	0.036	0.035	0.060	0.061	0.059	0.056	0.075	0.079	0.045	0.071
	0.6	0.073	0.071	0.076	0.070	0.072	0.035	0.035	0.055	0.055	0.055	0.057	0.072	0.077	0.047	0.075
	0.8	0.098	0.043	0.046	0.037	0.045	0.031	0.034	0.067	0.065	0.048	0.052	0.060	0.070	0.042	0.071
	0.9	0.173	0.027	0.030	0.024	0.032	0.024	0.022	0.111	0.097	0.052	0.058	0.035	0.041	0.042	0.065

Local GLS de-trended data; Case 3 (zero and seasonal frequency intercepts and trends)

N	θ_1	t_2	$\mathcal{MZ}_2$	$\mathcal{MZ}_{\pi_2}$	$\mathcal{MSB}_2$	$P_{2.T}$	$P_{12.T}$	$P_{012.T}$	F_{12}	F_{012}	$F^{D}_{\mathcal{M}.12}$	$F^{D}_{\mathcal{M}.012}$	$\mathcal{MSB}^{D}_{12}$	$\mathcal{MSB}^{D}_{012}$	$S^{D}_{\mathcal{M}.12}$	$S^{D}_{\mathcal{M}.012}$
50	0.0	0.043	0.035	0.040	0.034	0.041	0.023	0.019	0.062	0.069	0.031	0.027	0.038	0.035	0.037	0.033
	0.2	0.054	0.063	0.067	0.058	0.067	0.027	0.018	0.062	0.070	0.037	0.026	0.048	0.036	0.039	0.030
	0.4	0.068	0.084	0.088	0.081	0.090	0.033	0.018	0.061	0.072	0.042	0.029	0.056	0.037	0.044	0.031
	0.6	0.076	0.076	0.082	0.071	0.088	0.041	0.017	0.082	0.090	0.049	0.031	0.062	0.032	0.054	0.033
	0.8	0.121	0.068	0.072	0.064	0.077	0.035	0.011	0.112	0.122	0.066	0.046	0.048	0.015	0.063	0.038
	0.9	0.228	0.133	0.136	0.130	0.142	0.030	0.004	0.202	0.207	0.124	0.098	0.055	0.007	0.101	0.058
100	0.0	0.049	0.047	0.048	0.047	0.052	0.020	0.023	0.054	0.060	0.039	0.037	0.039	0.044	0.041	0.041
	0.2	0.051	0.057	0.058	0.056	0.062	0.025	0.021	0.054	0.058	0.038	0.035	0.049	0.044	0.041	0.039
	0.4	0.059	0.067	0.069	0.066	0.073	0.028	0.021	0.052	0.055	0.044	0.035	0.054	0.041	0.048	0.039
	0.6	0.065	0.059	0.061	0.058	0.065	0.034	0.022	0.065	0.062	0.055	0.041	0.059	0.044	0.058	0.044
	0.8	0.081	0.018	0.019	0.017	0.025	0.018	0.013	0.071	0.073	0.039	0.033	0.025	0.023	0.043	0.033
	0.9	0.166	0.025	0.026	0.023	0.029	0.013	0.004	0.130	0.125	0.052	0.042	0.017	0.006	0.046	0.031

https://doi.org/10.1017/S0266466617000135 Published online by Cambridge University Press

TABLE 5A. Empirical size of harmonic frequency unit root tests. MAIC lag selection. Order selection based on MAIC

DGP (5.1) with $c = 0$ and $u_{4n+s} = \varepsilon_{4n+s} + \theta_2 \varepsilon_{4n+s-2}$. Local GLS de-trended data; Case 1 (zero and seasonal frequency intercepts)

N	θ_2	F_1	F_{12}	F_{012}	$F^{\mathrm{D}}_{\mathcal{M}.1}$	$F^{\mathrm{D}}_{\mathcal{M}.12}$	$F^{\mathrm{D}}_{\mathcal{M}.012}$	$\mathcal{MSB}^{\mathrm{D}}_{1}$	$\mathcal{MSB}^{\mathrm{D}}_{12}$	$\mathcal{MSB}^{\mathrm{D}}_{012}$	$P_{1.T}$	$P_{12.T}$	$P_{012.T}$
50	0.00	0.055	0.065	0.071	0.048	0.058	0.061	0.075	0.096	0.115	0.067	0.040	0.047
	0.04	0.053	0.057	0.063	0.054	0.060	0.059	0.080	0.092	0.112	0.072	0.043	0.043
	0.16	0.052	0.054	0.054	0.064	0.067	0.066	0.104	0.099	0.118	0.093	0.047	0.046
	0.36	0.051	0.061	0.071	0.060	0.080	0.093	0.105	0.124	0.154	0.100	0.061	0.067
	0.64	0.069	0.068	0.067	0.049	0.070	0.086	0.123	0.131	0.156	0.127	0.064	0.069
	0.81	0.116	0.119	0.120	0.050	0.094	0.124	0.121	0.135	0.163	0.146	0.080	0.084
100	0.00	0.044	0.050	0.051	0.048	0.049	0.051	0.060	0.062	0.072	0.056	0.031	0.032
	0.04	0.050	0.048	0.050	0.052	0.051	0.051	0.067	0.060	0.068	0.064	0.030	0.031
	0.16	0.046	0.049	0.050	0.049	0.053	0.053	0.069	0.069	0.077	0.064	0.033	0.034
	0.36	0.042	0.047	0.050	0.056	0.063	0.068	0.074	0.072	0.081	0.071	0.038	0.039
	0.64	0.055	0.052	0.053	0.046	0.056	0.062	0.092	0.087	0.094	0.092	0.045	0.046
	0.81	0.082	0.077	0.076	0.025	0.045	0.060	0.081	0.090	0.094	0.100	0.050	0.049

N	θ_2	$S^{\mathrm{D}}_{\mathcal{M}.1}$	$S^{\mathrm{D}}_{\mathcal{M}.12}$	$S^{\mathrm{D}}_{\mathcal{M}.012}$	$\mathcal{Re}$-$\mathcal{MZ}_1$	$\mathcal{Re}$-$\mathcal{MSB}_1$	$\mathcal{Re}$-$\mathcal{MZ}_{t_1}$	$\mathcal{Im}$-$\mathcal{MZ}_1$	$\mathcal{Im}$-$\mathcal{MSB}_1$	$\mathcal{Im}$-$\mathcal{MZ}_{t_1}$
50	0.00	0.062	0.055	0.109	0.052	0.052	0.052	0.055	0.054	0.058
	0.04	0.069	0.063	0.114	0.062	0.062	0.062	0.057	0.057	0.059
	0.16	0.090	0.070	0.122	0.070	0.069	0.070	0.073	0.073	0.075
	0.36	0.090	0.087	0.159	0.065	0.063	0.066	0.064	0.066	0.065
	0.64	0.095	0.091	0.168	0.046	0.043	0.048	0.050	0.052	0.044
	0.81	0.093	0.105	0.196	0.035	0.032	0.038	0.036	0.039	0.031
100	0.00	0.052	0.039	0.064	0.053	0.051	0.052	0.050	0.050	0.051
	0.04	0.060	0.044	0.070	0.055	0.055	0.055	0.053	0.054	0.055
	0.16	0.058	0.047	0.075	0.052	0.052	0.054	0.050	0.049	0.051
	0.36	0.065	0.053	0.084	0.055	0.056	0.056	0.058	0.059	0.058
	0.64	0.073	0.057	0.094	0.050	0.046	0.053	0.049	0.049	0.047
	0.81	0.058	0.052	0.091	0.017	0.014	0.020	0.018	0.021	0.014

https://doi.org/10.1017/S0266466617000135 Published online by Cambridge University Press

TABLE 5B. Empirical size of harmonic frequency unit root tests. MAIC lag selection. Order selection based on MAIC

DGP (5.1) with $c = 0$ and $u_{4n+s} = \varepsilon_{4n+s} + \theta_2 \varepsilon_{4n+s-2}$. Local GLS de-trended data; Case 3 (zero and seasonal frequency intercepts and trends)

N	θ_2	F_1	F_{12}	F_{012}	$F^{\mathrm{D}}_{\mathcal{M}.1}$	$F^{\mathrm{D}}_{\mathcal{M}.12}$	$F^{\mathrm{D}}_{\mathcal{M}.012}$	$\mathcal{MSB}^{\mathrm{D}}_{1}$	$\mathcal{MSB}^{\mathrm{D}}_{12}$	$\mathcal{MSB}^{\mathrm{D}}_{012}$	$P_{1.T}$	$P_{12.T}$	$P_{012.T}$
50	0.00	0.048	0.059	0.068	0.028	0.028	0.026	0.033	0.034	0.037	0.044	0.021	0.022
	0.04	0.063	0.068	0.070	0.042	0.035	0.028	0.045	0.036	0.032	0.060	0.021	0.019
	0.16	0.067	0.070	0.069	0.056	0.046	0.037	0.067	0.044	0.032	0.085	0.030	0.020
	0.36	0.070	0.090	0.109	0.059	0.063	0.064	0.081	0.066	0.068	0.101	0.043	0.043
	0.64	0.113	0.122	0.130	0.072	0.072	0.069	0.106	0.061	0.047	0.133	0.044	0.027
	0.81	0.246	0.250	0.259	0.036	0.036	0.036	0.174	0.043	0.030	0.202	0.036	0.018
100	0.00	0.046	0.052	0.057	0.036	0.036	0.036	0.039	0.042	0.044	0.044	0.023	0.022
	0.04	0.052	0.053	0.054	0.043	0.041	0.034	0.052	0.041	0.038	0.054	0.023	0.021
	0.16	0.053	0.060	0.064	0.047	0.049	0.049	0.059	0.056	0.052	0.065	0.031	0.028
	0.36	0.054	0.060	0.063	0.055	0.057	0.057	0.066	0.059	0.060	0.072	0.033	0.033
	0.64	0.079	0.079	0.081	0.041	0.047	0.049	0.062	0.059	0.056	0.076	0.034	0.032
	0.81	0.160	0.146	0.143	0.031	0.044	0.045	0.052	0.040	0.034	0.066	0.023	0.017

N	θ_2	$S^{\mathrm{D}}_{\mathcal{M}.1}$	$S^{\mathrm{D}}_{\mathcal{M}.12}$	$S^{\mathrm{D}}_{\mathcal{M}.012}$	$\mathcal{Re}$-$\mathcal{MZ}_1$	$\mathcal{Re}$-$\mathcal{MSB}_1$	$\mathcal{Re}$-$\mathcal{MZ}_{t_1}$	$\mathcal{Im}$-$\mathcal{MZ}_1$	$\mathcal{Im}$-$\mathcal{MSB}_1$	$\mathcal{Im}$-$\mathcal{MZ}_{t_1}$
50	0.00	0.028	0.032	0.032	0.031	0.030	0.032	0.031	0.031	0.031
	0.04	0.042	0.040	0.033	0.037	0.036	0.037	0.036	0.037	0.036
	0.16	0.059	0.051	0.042	0.044	0.043	0.045	0.045	0.047	0.044
	0.36	0.066	0.072	0.074	0.041	0.039	0.042	0.040	0.042	0.038
	0.64	0.085	0.078	0.070	0.034	0.032	0.035	0.039	0.040	0.037
	0.81	0.036	0.039	0.042	0.035	0.034	0.036	0.037	0.039	0.036
100	0.00	0.036	0.039	0.042	0.035	0.034	0.036	0.037	0.039	0.036
	0.04	0.045	0.044	0.038	0.040	0.039	0.040	0.040	0.039	0.040
	0.16	0.050	0.054	0.053	0.041	0.040	0.042	0.040	0.040	0.039
	0.36	0.060	0.062	0.062	0.047	0.046	0.049	0.046	0.047	0.045
	0.64	0.050	0.053	0.052	0.021	0.019	0.023	0.019	0.020	0.018
	0.81	0.039	0.042	0.038	0.013	0.013	0.014	0.012	0.013	0.012

significantly better size control than the HEGY t_0 test, and show more pronounced improvements in relative size control than the HEGY tests as the sample size increases. In the example above, the three $\mathcal{M}$ tests all display empirical size of around 8% for $N = 50$, with no over-sizing seen for $N = 100$; indeed, again consistent with the simulation results in Ng and Perron (2001), the tests are all slightly under-sized in the latter case. As with the t_0 test, distortions tend to be lower under Case 3 (with the exception of the case where $\theta_1 = 0.9$ and $N = 50$); here the three $\mathcal{M}$ tests for $\theta_1 = 0.9$ are again slightly under-sized when $N = 100$ (compared to 17% size for t_0). The feasible point optimal $P_{0,T}$ test of Rodrigues and Taylor (2007) behaves very similarly to the three $\mathcal{M}$ tests. Similar observations can be made about the joint frequency tests in Table 1. The lowest size distortions are again displayed by the $\mathcal{M}$ tests from Section 3 and the corresponding feasible point optimal test, $P_{012,T}$, from Rodrigues and Taylor (2007), although the latter is consistently undersized, especially so under Case 3. In particular, the $F^{\mathrm{D}}_{\mathcal{M},012}$ test displays consistently better size control than the HEGY F_{012} test.

Turning to the results for the Nyquist frequency in Tables 4a (Case 1) and 4b (Case 3), very similar patterns of size distortions are seen here as were observed in Table 3 as might be expected, given that an equivalent near cancellation effect is obtained here for a given value of θ_1 as for the zero frequency results. In addition to the joint tests considered in Table 3, Tables 4a and 4b also report the joint tests for testing the null hypothesis of unit roots at all of the seasonal frequencies, $H_{0,\mathrm{seas}}$. Again the same relative behaviour is seen between the HEGY-type and $\mathcal{M}$-type tests as is observed for the other tests.

Finally, we turn to the results for the seasonal harmonic frequency in Tables 5a and 5b. Consider first the results for Case 1 in Table 5a. As with the results for the HEGY tests in Tables 3 and 4a–4b, the harmonic frequency HEGY F_1 test displays good size control for small values of θ_2 but is again rather over-sized for the larger values of θ_2 considered. For example, for $\theta_2 = 0.81$ and $N = 50$ the F_1 test has size of about 12% falling to about 8% for $N = 100$. The best size control is offered by the $F^{\mathrm{D}}_{\mathcal{M},1}$ test which displays excellent size control for all values of θ_2 considered for both $N = 50$ and $N = 100$. In the example above $F^{\mathrm{D}}_{\mathcal{M},1}$ has empirical size of about 5% for $N = 50$ and 3% for $N = 100$. The single root demodulated tests $\mathcal{R}e\text{-}\mathcal{MZ}_1$, $\mathcal{I}m\text{-}\mathcal{MZ}_1$, $\mathcal{R}e\text{-}\mathcal{MZ}_{t_1}$, $\mathcal{I}m\text{-}\mathcal{MZ}_{t_1}$, $\mathcal{R}e\text{-}\mathcal{MSB}_1$ and $\mathcal{I}m\text{-}\mathcal{MSB}_1$, perform similarly to one another but do not control size as well as $F^{\mathrm{D}}_{\mathcal{M},1}$, displaying significant under-sizing when $\theta_2 = 0.81$, and some over-sizing for $\theta_2 = 0.16$ when $N = 50$. The $\mathcal{MSB}^{\mathrm{D}}_1$ and $P_{1,T}$ test of Rodrigues and Taylor (2007) behave similarly to one another, displaying slightly poorer size control than the HEGY F_1 test. As regards the joint frequency tests, here the feasible point optimal tests of Rodrigues and Taylor (2007) appear to offer the best size control overall. The joint frequency $\mathcal{M}$-type tests perform similarly to the corresponding joint frequency HEGY tests, F_{12} and F_{012}.

The results in Table 5b for Case 3 show a similar ordering of the tests as for Case 1 but with an overall deterioration seen in the finite sample size control of most of the tests. Again the best size control is shown by the $F^{\mathrm{D}}_{\mathcal{M},1}$ test, which

https://doi.org/10.1017/S0266466617000135 Published online by Cambridge University Press

displays fairly similar size control overall to the single root demodulated tests. These tests again display considerably better size control in the near cancellation region than the HEGY F_1 test. To illustrate when $\theta_2 = 0.81$, the HEGY F_1 test has empirical size of about 25% for $N = 50$ and 16% for $N = 100$, while the empirical sizes of $F^{\mathrm{D}}_{\mathcal{M},1}$ in these cases are about 4% and 3%, respectively, and those of the $P_{1,T}$ test are about 20% and 7%, respectively. In the case of the joint frequency tests, the joint frequency $\mathcal{M}$-type tests display arguably the best overall size control, now notably better than the corresponding joint frequency HEGY tests. The feasible point optimal tests of Rodrigues and Taylor (2007) also avoid any over-sizing but display a stronger tendency to under-sizing than the $\mathcal{M}$ tests.

5.2. Empirical Power

Figures 3–6 graph the finite sample size adjusted (to 5%) power functions of the tests[5] for the case where the data are generated according to (5.1) with

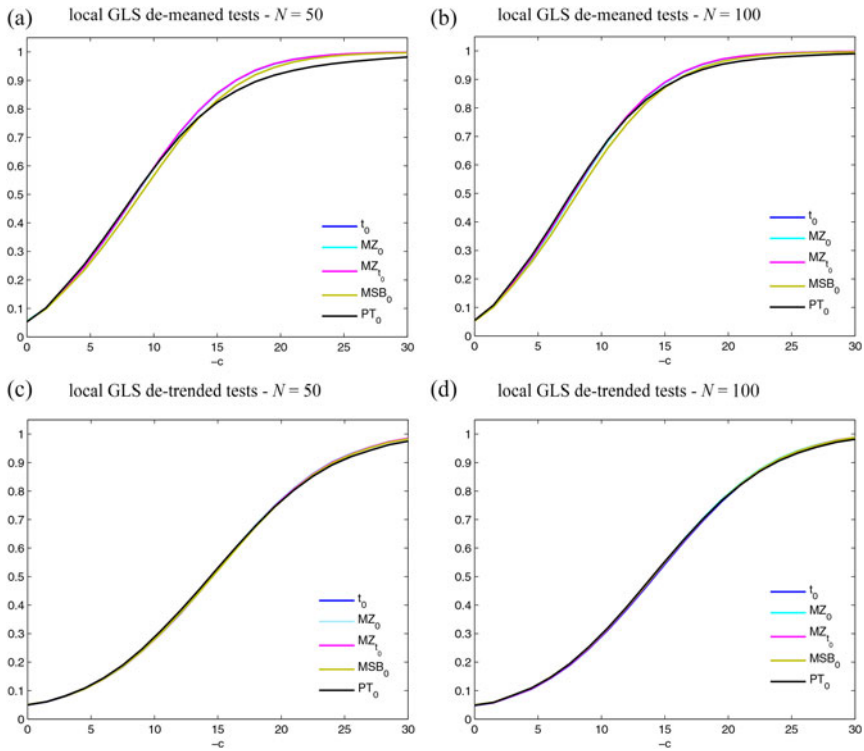


FIGURE 3. Finite sample size-adjusted power functions of zero frequency unit root tests (quarterly case, $S = 4$).

https://doi.org/10.1017/S0266466617000135 Published online by Cambridge University Press

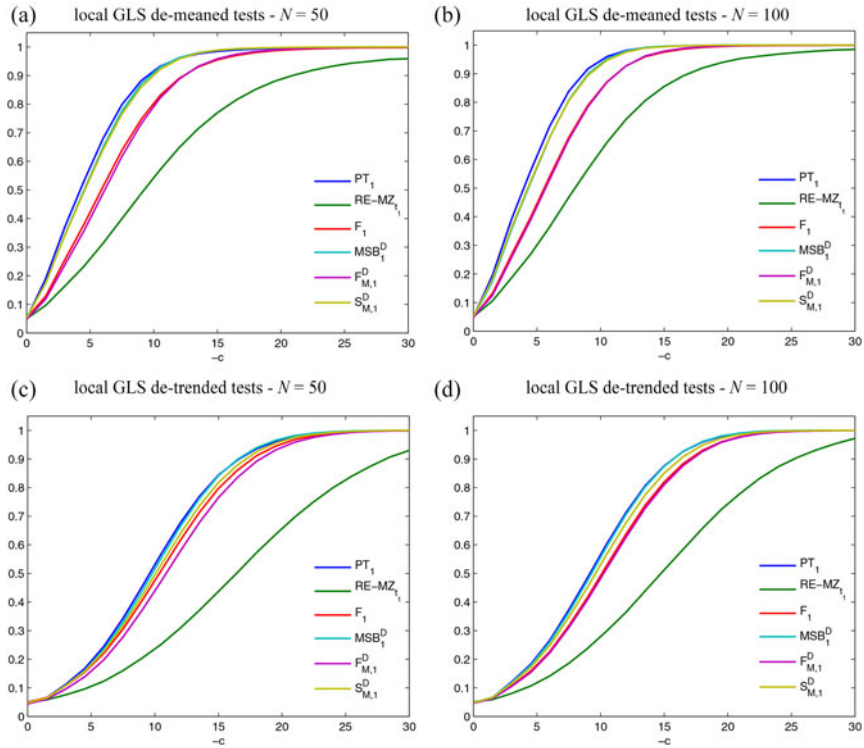


FIGURE 4. Finite sample size-adjusted power functions of harmonic frequency unit root tests (quarterly case, $S = 4$).

$u_{4n+s} \sim NIID(0,1)$, with K commensurately set to zero in the formula for $k_{\max K}$. And as in Rodrigues and Taylor (2007) the power results pertain to the case where, when moving a particular noncentrality parameter c_k, $k = 0, 1, 2$ away from unity, the remaining noncentrality parameters are all held at zero. The index, c, on the horizontal axes of the graphs has the same meaning as described above for Figures 1 and 2.

From Figure 3 we observe that the zero frequency tests display very similar power, particularly under local GLS de-trending (Case 3) where, even for $N = 50$, the power functions of the various tests are almost indistinguishable. In the case of local GLS de-meaning (Case 1) and for the smaller sample size, $N = 50$, and as we move further into the stationarity region (i.e., as c becomes more negative) we note that the point optimal test, PT_0, loses some power relative to the other tests, but overall finite sample power remains very similar across the tests.

Turning to the results for the harmonic frequency unit root tests reported in Figure 4 we see that, in line with the corresponding asymptotic local power results reported in Figure 1, there is rather more variation across the finite sample power properties of the various tests, relative to the results for the zero frequency

https://doi.org/10.1017/S0266466617000135 Published online by Cambridge University Press

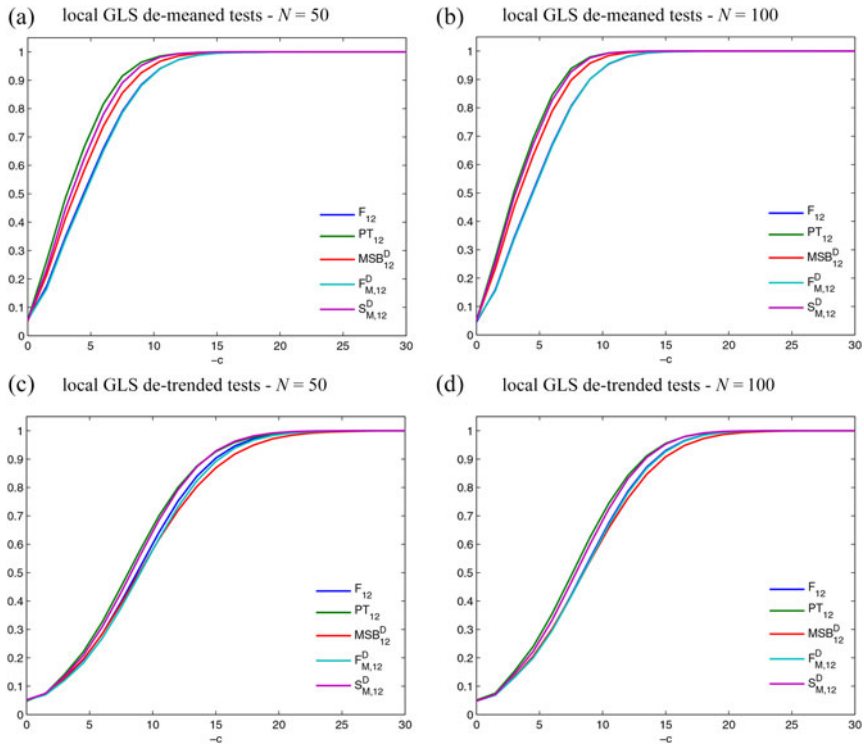


FIGURE 5. Finite sample size-adjusted power functions of joint seasonal frequency tests (quarterly case, $S = 4$).

tests in Figure 3. Again consistent with the corresponding asymptotic local power results in Figures 1(c) and 1(d), we see in Figure 4 that the demodulated single unit root test $\mathcal{R}e{-}\mathcal{M}\mathcal{Z}_{t_1}$ (again we only report one of these demodulated single unit root tests because they display virtually identical power properties) displays considerably lower power than the other harmonic frequency unit root tests. As for the remaining tests, under Case 1 the best performing tests are PT_1, $\mathcal{MSB}_1^D$ and $\mathcal{S}_{M,1}^D$, all outperforming the F_1 and $F_{M,1}^D$ tests, which perform very similarly, on power. These rankings hold for both $N = 50$ and $N = 100$; indeed, the local power properties of a given test alter little between the two sample sizes, suggesting again that the asymptotic local power functions provide good predictors for the finite sample powers of the tests. Under Case 3, roughly the same power ordering as was observed for Case 1 is seen, although again as predicted by the asymptotic local power functions, the power differentials between the tests are decreased relative to those seen under Case 1.

We turn now to the joint frequency tests. Consider first the joint seasonal unit root tests graphed in Figure 5. For both sample sizes and under both Cases 1 and 3 we see that the differences across the various power functions are relatively small.

https://doi.org/10.1017/S0266466617000135 Published online by Cambridge University Press

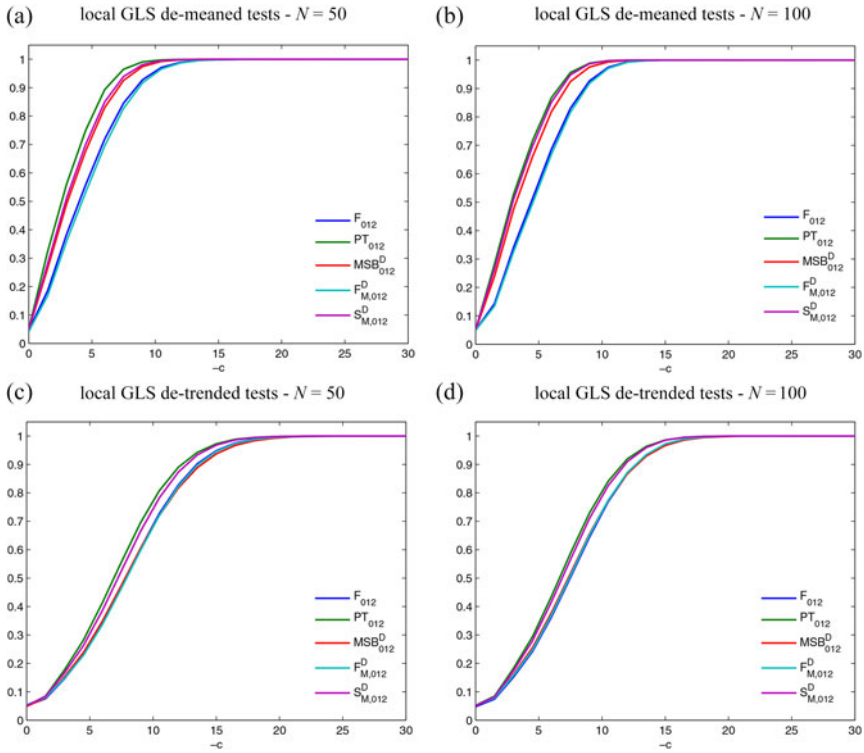


FIGURE 6. Finite sample size-adjusted power functions of joint zero and seasonal frequency tests (quarterly case, $S = 4$).

In terms of relative performance, under Case 1, for both sample sizes the highest power is delivered by PT_{12}, closely followed by $\mathcal{S}^D_{M,12}$ and $\mathcal{MSB}^D_{12}$, with the lowest power displayed by F_{12} and $F^D_{M,12}$, the latter two displaying almost identical power. Under Case 3, we again see that the best performing tests on power are PT_{12} and $\mathcal{S}^D_{M,12}$, while the power performances of F_{12} and $F^D_{M,12}$ are now as good and sometimes superior to that of $\mathcal{MSB}^D_{12}$. Next in Figure 6 we display finite sample power graphs for the tests of the null hypothesis of a unit root at all of the zero and seasonal frequencies. The conclusions from these graphs are qualitatively similar to those remarked on above for the joint seasonal frequency unit root tests. The only exception is for local GLS de-trending, where it is observed that F_{012}, $F^D_{M,012}$, and $\mathcal{MSB}^D_{012}$ display almost identical finite sample power.

For completeness, Figures S.1–S.4 in the Supplementary Appendix report the corresponding size *unadjusted* power results for tests based on the relevant asymptotic critical values. They highlight a degree of over-sizing seen in some of the tests, particularly the augmented HEGY tests, making meaningful power comparisons between the tests somewhat difficult when not using size adjusted power.

https://doi.org/10.1017/S0266466617000135 Published online by Cambridge University Press

Interestingly, the point optimal tests of Rodrigues and Taylor (2007), which were already seen in Section 5.1 to show a tendency to undersize, are correspondingly seen to lack power in cases where they are under-sized relative to the other tests when comparisons are made on the basis of size unadjusted power. This would seem to further strengthen the case for the use of the $\mathcal{M}$-type tests in that they simultaneously control size well, in general, and yet avoid the low power that can be seen with the point optimal tests in small samples.

6. CONCLUSIONS

We have generalised the so-called $\mathcal{M}$ class of semiparametric unit root tests to allow for unit root testing at the zero and seasonal frequencies in seasonally observed data. For tests involving the seasonal harmonic frequencies this was shown to necessitate the use of demodulated data. In the nonseasonal case the $\mathcal{M}$ unit root tests, combined with an autoregressive spectral density-based estimator of the long run variance, are known to considerably improve on the finite sample size control of augmented Dickey-Fuller tests in the most problematic (near-cancellation) case where the driving shocks contain a strong negative moving average component. Using Monte Carlo simulation methods we have shown that this result carries over to the seasonal case with the $\mathcal{M}$-type seasonal unit root tests we develop here displaying significantly better finite sample size control than the corresponding parametric HEGY seasonal unit root tests in near cancellation regions. As in the nonseasonal case, these improvements in finite sample size were shown not to come at the expense of any loss in power relative to the HEGY tests. Moreover, certain of the $\mathcal{M}$-type seasonal unit root tests were shown to achieve similar or better finite-sample power properties than the feasible point optimal tests of Rodrigues and Taylor (2007).

Overall, based on both the finite sample size and local power properties of the tests considered, we recommend the use of either one of the trinity of $\mathcal{M}$-type tests or the feasible point optimal test of Rodrigues and Taylor (2007), when testing for a unit root at either the zero or Nyquist frequencies. For testing for a complex pair of unit roots at one of the seasonal harmonic frequencies, we recommend the test based on $F^{D}_{M,1}$ of (3.19), because among the tests considered it was the only one which delivered reliable size control. In each case we recommend basing these test statistics on an autoregressive spectral density (seasonal) long run variance estimator using del Barrio Castro et al. (2016) seasonal implementation of the MAIC lag selection criterion of Ng and Perron (2001).

NOTES

1. The term $-T^{-1}(y_0^{\xi})^2$ can be omitted from the numerator of $\mathcal{MZ}_0$ for the case of local GLS de-trended data; see Müller and Elliott (2003).

2. An alternative approach is to define $\mathcal{M}$ tests at the harmonic frequencies analogously to the zero and Nyquist frequency $\mathcal{MZ}_k$, $\mathcal{MSB}_k$ and $\mathcal{MZ}_{t_k}$ $k = 0, S/2$, tests outlined above, using the relevant filtered variables $y^{\xi}_{k,Sn+s}$ and $y^{*\xi}_{k,Sn+s}$, $k = 1, \ldots, S^*$ defined just below (2.4). Monte Carlo

https://doi.org/10.1017/S0266466617000135 Published online by Cambridge University Press

simulation results reported in the accompanying working paper, del Barrio Castro, Rodrigues, and Taylor (2015), suggest, however, that this approach yields tests with inferior finite sample size properties to the standard augmented HEGY tests.

3. The seasonal unit root tests of Jansson and Nielsen (2011) have asymptotic local power functions which are almost indistinguishable from the point optimal tests and, hence, are not reported.

4. The relevant HEGY tests t_k, $k = 0, S/2$, are not included in Figures 1(a) and 1(b) because they are asymptotically equivalent to $\mathcal{M}Z_{t_k}$; cf. Remark 4.2.

5. Results are not reported here for the corresponding Nyquist frequency unit root tests because they were almost identical to the corresponding zero frequency tests reported in Figure 3.

REFERENCES

del Barrio Castro, T., D.R. Osborn, & A.M.R. Taylor (2016) The performance of lag selection and detrending methods for HEGY seasonal unit root tests. *Econometric Reviews* 35, 122–168.

del Barrio Castro, T., P.M.M. Rodrigues, & A.M.R. Taylor (2015) Semi-Parametric Seasonal Unit Root Tests. Essex Finance Centre Working Paper Series number 16807. Available at http://repository.essex.ac.uk/16807/.

Berk, K.N. (1974) Consistent autoregressive spectral estimates. *The Annals of Statistics* 2, 389–502.

Bhargava, A. (1986) On the theory of testing for unit roots in observed time series. *Review of Economic Studies* 53, 369–384.

Box, G.E.P. & G.M. Jenkins (1976) *Time Series Analysis: Forecasting and Control*, Revised ed. Holden-Day.

Breitung, J. & P.H. Franses (1998) On Phillips-Perron type tests for seasonal unit roots. *Econometric Theory* 14, 200–221.

Elliott, G., T.J. Rothenberg, & J.H. Stock (1996) Efficient tests for an autoregressive unit root. *Econometrica* 64, 813–836.

Ghysels, E. & D.R. Osborn (2001) *The Econometric Analysis of Seasonal Time Series*. CUP.

Granger, C.W.J. & M. Hatanaka (1964) *Spectral Analysis of Economic Time Series*. Princeton University Press.

Gregoir, S. (1999) Multivariate time series with various hidden unit roots, Part I: Integral operator algebra and representation theory. *Econometric Theory* 15, 435–468.

Gregoir, S. (2006) Efficient tests for the presence of a pair of complex conjugate unit roots in real time series. *Journal of Econometrics* 130, 45–100.

Haldrup, N. & M. Jansson (2006) Improving power and size in unit root testing. In T.C. Mills & K. Patterson (eds.), *Palgrave Handbooks of Econometrics: Vol. 1 Econometric Theory, Chapter 7*, pp. 252–277. Palgrave MacMillan.

Hylleberg, S., R.F. Engle, C.W.J. Granger, & B.S. Yoo (1990) Seasonal integration and cointegration. *Journal of Econometrics* 44, 215–238.

Jansson, M. (2002) Consistent covariance matrix estimation for linear processes. *Econometric Theory* 18, 1449–1459.

Jansson, M. & M.Ø. Nielsen (2011) Nearly efficient likelihood ratio tests for seasonal unit roots. *Journal of Time Series Econometrics* 3(1), Article 5, 1–19.

Müller, U.K. & G. Elliott (2003) Tests for unit roots and the initial condition. *Econometrica* 71, 1269–1286.

Ng, S. & P. Perron (2001) Lag length selection and the construction of unit root tests with good size and power. *Econometrica* 69, 1519–1554.

Perron, P. & Z. Qu (2007) A simple modification to improve the finite sample properties of Ng and Perrons unit root tests. *Economics Letters* 94, 12–19.

Perron, P. & S. Ng (1996) Useful modifications to some unit root tests with dependent errors and their local asymptotic properties. *Review of Economic Studies* 63, 435–463.

Perron, P. & S. Ng (1998) An autoregressive spectral density estimator at frequency zero for nonstationarity tests. *Econometric Theory* 14, 560–603.

https://doi.org/10.1017/S0266466617000135 Published online by Cambridge University Press

Phillips, P.C.B. & P. Perron (1988) Testing for a unit root in time series regression. *Biometrika* 75, 335–346.

Rodrigues, P.M.M. & A.M.R. Taylor (2007) Efficient tests of the seasonal unit root hypothesis. *Journal of Econometrics* 141, 548–573.

Smith, R.J., Taylor, A.M.R., & T. del Barrio Castro (2009) Regression-based seasonal unit root tests. *Econometric Theory* 25, 527–560.

Stock, J.H. (1999) A class of tests for integration and cointegration. In R.F. Engle & H. White (eds.), *Cointegration, Causality and Forecasting. A Festschrift in Honour of Clive W.J. Granger*, pp. 137–167. Oxford University Press.

https://doi.org/10.1017/S0266466617000135 Published online by Cambridge University Press